Pion Photoproduction and Compton Scattering in the Resonance Region

R. Kajikawa

Department of Physics
Nagoya University
Nagoya 464, Japan

In this review, I will concentrate my discussion on the present status of classical (s=0) nucleon spectroscopy studied with the low energy real and virtual photons as follows:

I. Photocoupling of Nucleon Resonance ($Q^2=0$)
   1. New data on pion and eta photoproduction
      proton target: $\gamma p \to \pi^+ n$, $\pi^o p$, $\eta^o p$
      neutron target: $\gamma n \to \pi^- p$
   2. Recent phenomenological analyses
   3. Comparison with quark models
   4. New data on Compton scattering

II. γ_v-Coupling of Nucleon Resonance ($Q^2>0$)
   1. New data on electroproduction
      proton target: $\gamma_v p \to \pi^+ n$, $\pi^o p$
      neutron target: $R = \frac{ed \to e\pi^- p(p)}{ed \to e\pi^+ n(n)} \simeq \frac{\gamma_v n \to \pi^- p}{\gamma_v p \to \pi^+ n}$
   2. Multipole analyses and comparison with quark models

I. Photocoupling of Nucleon Resonance ($Q^2=0$)

In order to determine photocouplings of nucleon resonances, the pion photoproduction $\gamma N \to \pi N$ is the most suitable process because a large fraction of the process occurs through the resonance formation and in addition the πN partial widths are well known for many resonances. However, the existence of appreciable non-resonant (background) production still makes the separation of indivivual resonance contributions a rather complicated matter comparing to the πN elastic scattering where the background contribution is smaller and the measurements are easier. To determine production amplitudes in model-independent ways, we need 7 independent measurements for each process, and for isospin decomposition we need at least 3 processes, e.g. $\gamma p \to \pi^+ n$, $\pi^o p$ and $\gamma n \to \pi^- p$. Obviously we need a great deal of data for all the observables and an extensive phenomenological analysis in which all known resonances are properly parametrized using the knowledge obtained from the most recent πN partial wave analysis. In fact, as the blanks in data maps are filled with new data, the photocouplings determined by subsequent analyses have become more and more accurate and in addition agree better with each other. As the quark model has also been improved in recent years, a quantitative comparison between the experiment and the theory can be made to determine theoretical parameters.

1. New data on pion and eta photoproduction

1-1. Observables and definitions

Throughout this chapter I will use the standard definition of observables and the notations given by Barker-Donnachie-Storrow [1]. In the single polarization measurement (S.P.M.), the following 4 observables are available;
- Differential cross section: $d\sigma/d\Omega$
- Recoil nucleon polarization: P
- Polarized beam asymmetry: Σ
- Polarized target asymmetry: T

The double polarization measurement (D.P.M.) supplies us with more observables;
- Beam and target polarization: G and H

- Beam and recoil nucleon polarization: Ox and Oz

The experimental conditions for these measurements are schematically illustrated in Fig. 1. With the D.P.M. technique, P, Σ and T are also obtained by a proper choice of experimental conditions.

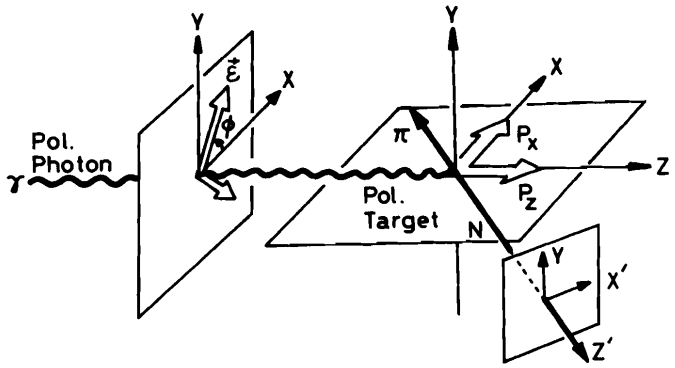

Fig. 1. Illustration of the double polarization measurements for the single pion photoproduction. $\vec{\varepsilon}$ represents the direction of the photon polarization, and Px etc. the nucleon polarization components. By the "beam-target" polarization experiments, G and H observables are obtained by setting $\phi=\pi/4$ and $-\pi/4$ respectively. The S.P.M. observables Σ, T, P are also available with $\phi=0$ or $\pi/2$. In the "beam-recoil nucleon" polarization experiments, P=Py, Ox=Px', Oz=Pz' observables are measured by $\phi=\pi/4$ and $-\pi/4$.

1-2. Quality of data

The recoil nucleon polarization P is measured with the double scattering method in the S.P.M., where the second target serves as a polarization analyzer. Different materials are chosen as the analyzer depending on the kinetic energy (T) of recoil nucleon; e.g. the liquid helium for T<80 MeV, the carbon 80<T<300 MeV and the liquid hydrogen for T ≥ 250 MeV, with the analyzing efficiency of about 0.5, 1-2 and 0.5 % respectively. Mainly due to this low efficiencies, the error in the P measurement is typically ±10 %.

The polarized beam asymmetry Σ is measured with a quasimonochromatic beam, a coherent bremsstrahlung, produced by electrons in a single crystal of silicon or diamond. The beam polarization available with this method is 40-60 %, but the useable photon energy is limited to 40 % or less of the primary energy. The overall error of final results is about ±3 %.

The target asymmetry T is measured with the butanol ($C_4H_{10}O$) or deuterized butanol ($C_4D_{10}O$) doped with paramagnetic impurities as the proton or deuteron target. The nucleon (deuteron) polarization is attained by the dynamical polarization method at the temperature of 0.1-0.5 K in the magnetic field of 2.5 T. The typical polarization is 65-70 % for protons and 17-35 % for neutrons. The resulting accuracy in T is about ±5 % including systematic errors.

The measurements of the D.P.M. observables G and H use a combination of two polarization techniques, and the typical errors in final result are about ±10 %. The extensive G and H measurements have been performed at Daresbury for the proton target, providing a substantial amount of data in the high energy region up to 2.3 GeV.

1-3. Present status of data accumulation

After the 1977 International Symposium on Lepton and Photon Interactions (DESY), the amount of data increased quite rapidly. I plotted all the available data points in Figs. 2a, b and c for $\gamma p \to \pi^+ n$, $\pi^0 p$ and $\gamma n \to \pi^- p$ respectively. The new data presented to this Symposium as well as those published since 1978 are listed in Tables 1a, b and c. Those data maps were first introduced by H. Fischer [2] at the Bonn Symposium in 1973 to illustrate apparent blanks in the

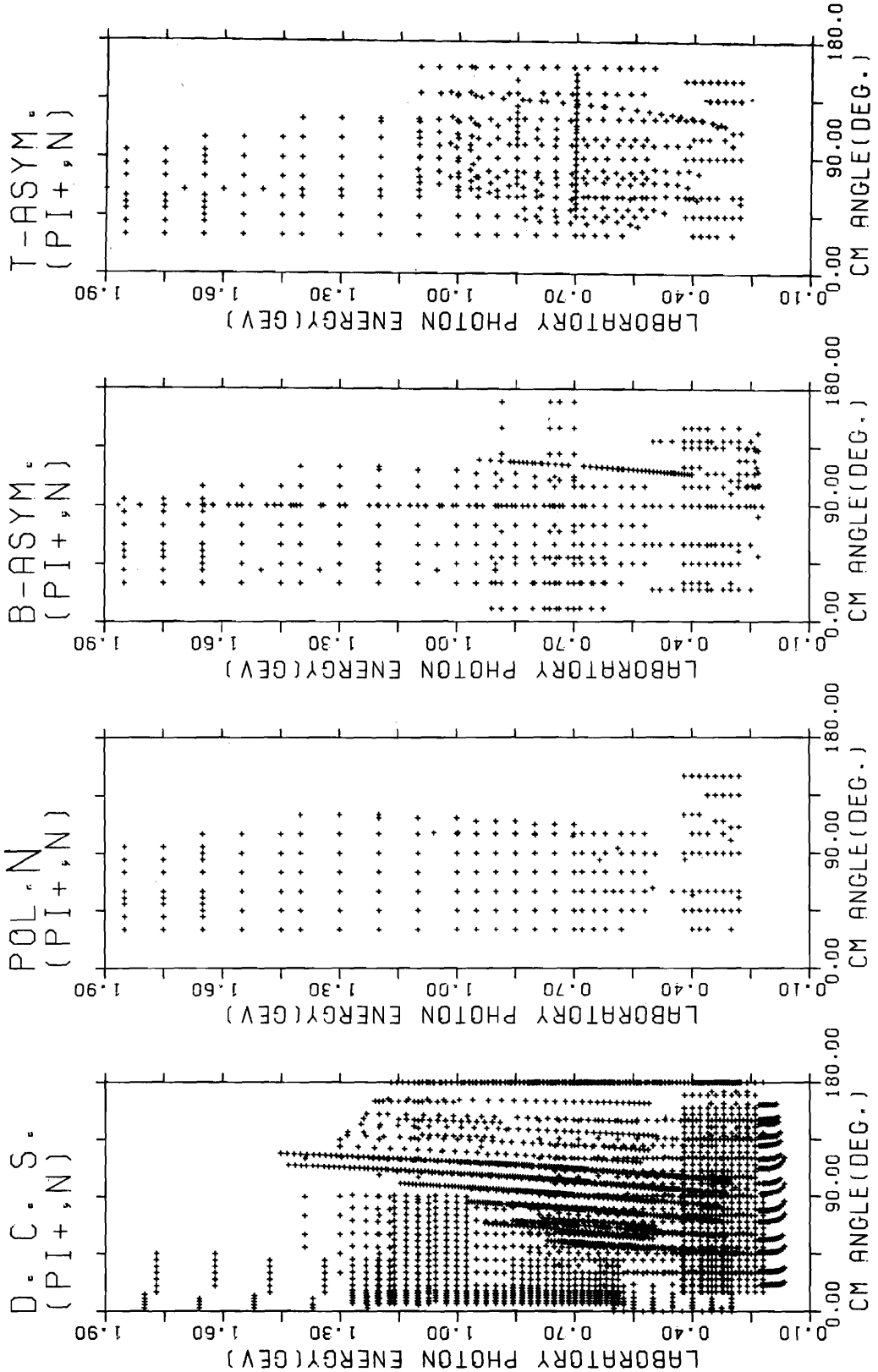

Fig. 2a. Data maps 1981 for 4 observables on $\gamma p \to \pi^+ n$. Data are taken from Ref.[81].

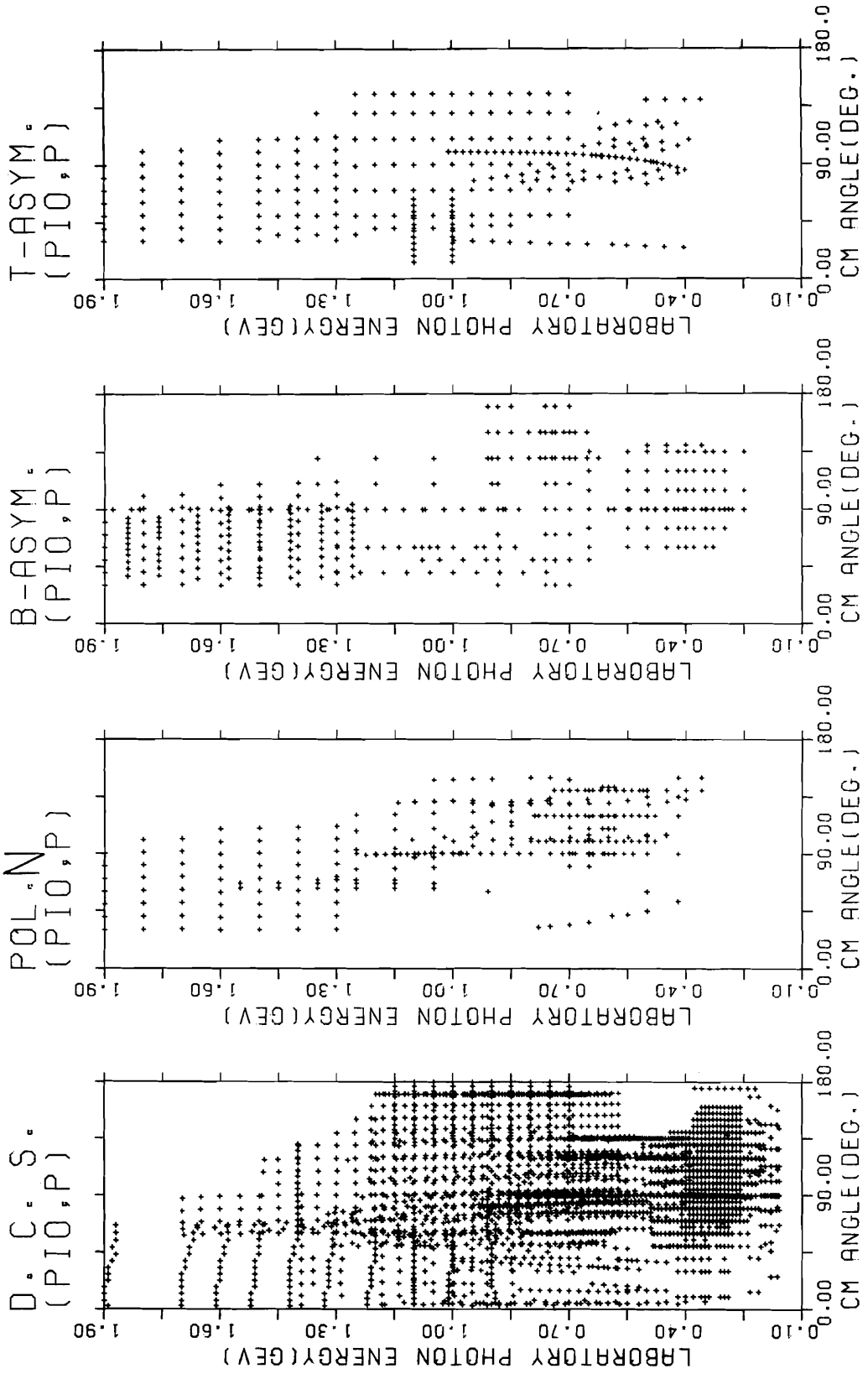

Fig. 2b. Data maps 1981 for 4 observables on $\gamma p \to \pi^0 p$. Data are taken from Ref.[81].

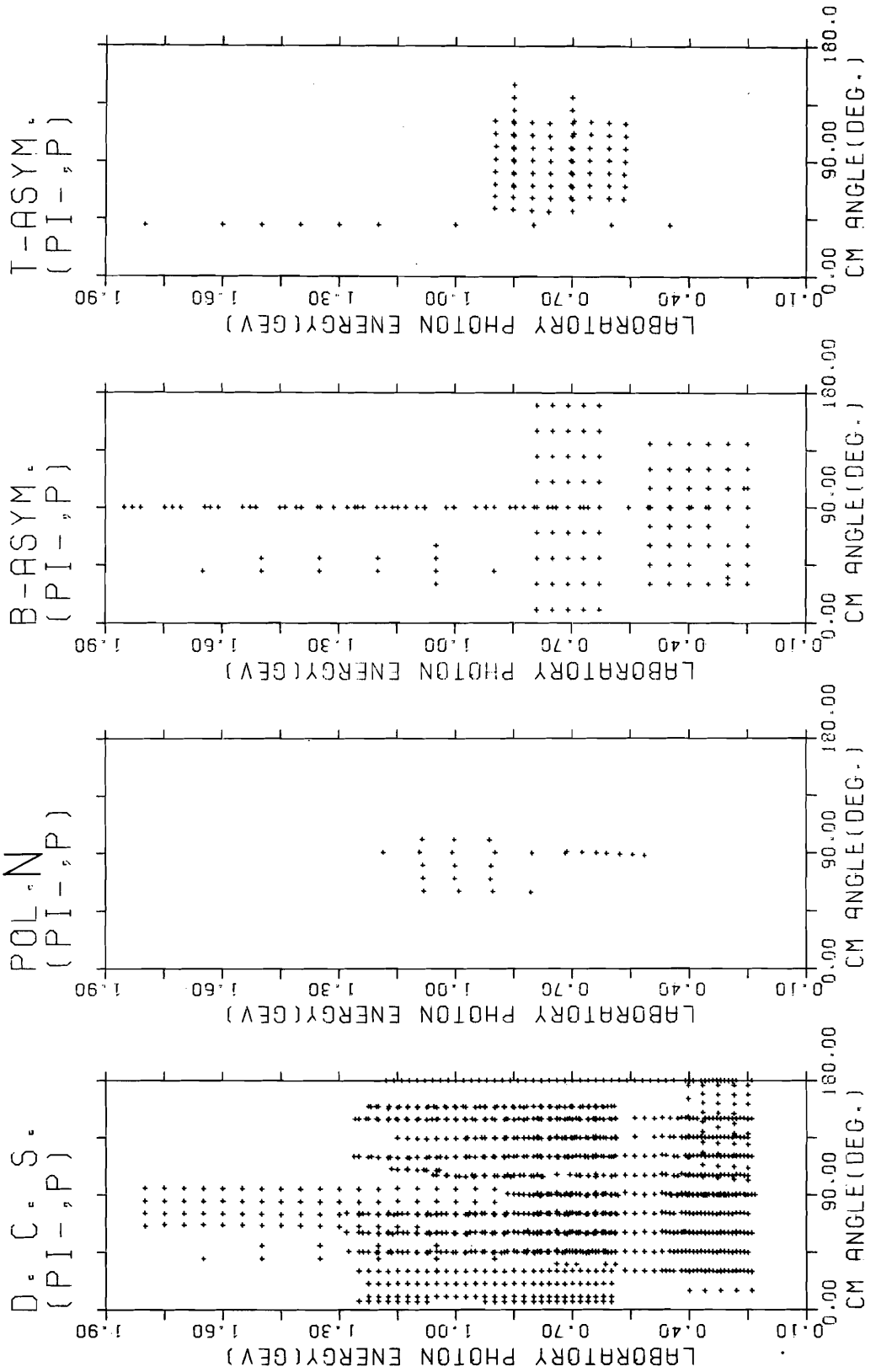

Fig. 2c. Data maps 1981 for 4 observables on $\gamma n \to \pi^- p$. Data are taken from Ref.[81].

data set, and, indeed, the amplitude analyses have been considerably improved as more blanks were filled in. It seems to me, however, that there is no extremely sensitive observable in the photocoupling determination.

Table 1a. New data ($\gamma p \to \pi^+ n$) since 1978

	Obs.	E_γ (MeV)	θ_{cm}	No. of data points	Institute
1	$d\sigma/d\Omega$	290 - 1940	45 - 130	705	Bonn 80 [3]
2	P	280 - 420	30 - 150	54	Kharkov 80 [4]
3	P	520 - 1650	30 - 120	130	Glasgow-Liv.-Sheff.79 [5]
4	P	700 - 1100	103 - 106	8	INS(Tokyo) 81 [6]
5	P	1650 - 2250	30 - 115	54	Glasgow-Liv.-Shell. 79 [5]
6	Σ	280 - 420	30 - 150	56	Kharkov 80 [4]
7	Σ	400 - 943	114 - 125	48	Bonn 80 [7]
8	Σ	520 - 1650	30 - 120	130	Glasgow-Liv.-Sheff. 79 [5]
9	Σ	900 - 1650	40	4	Yerevan 78 [8]
10	Σ	1650 - 2250	30 - 115	54	Glasgow-Liv.-Sheff.79 [5]
11	T	280 - 420	30 - 150	53	Kharkov 80 [4]
12	T	300 - 420	30 - 150	26	Kharkov 79 [9]
13	T	520 - 1650	30 - 120	130	Glasgow-Liv.-Sheff. 79 [5]
14	T	1650 - 2250	30 - 115	54	Glasgoe-Liv.-Sheff. 79 [5]
15	T	950 - 1100	70 - 160	32	Nagoya-Osaka 81 [10]
16	G	700 - 1875	40 - 100	77	Glasgow-Liv.-Sheff. 80 [11]
17	H	600 - 1775	40 - 100	77	Glasgow-Liv.-Sheff. 80 [11]

Table 1b. New data ($\gamma p \to \pi^0 p$) since 1978

	Obs.	E_γ (MeV)	θ_{cm}	No. of data points	Institute
1	$d\sigma/d\Omega$	290 - 360	10 - 90	30	Lebedev 78 [12]
2	$d\sigma/d\Omega$	596 - 1800	170	107	Bonn 79 [13]
3	$d\sigma/d\Omega$	1400	60 - 175	24	Bonn 79 [14]
4	P	480 - 800	100 - 140	47	Kharkov 78 [15]
5	P	450	105	1	Kharkov 79 [16]
6	P	400 - 1142	100 - 134	34	INS(Tokyo) 80 [17]
7	P	1300 - 2100	30 - 112	81	Glasgow-Liv.-Sheff. 79 [18]
8	P	400 - 750	150, 160	14	INS(Tokyo) 81 [19]
9	Σ	760 - 1300	40 - 50	15	Yerevan 79 [20]
10	Σ	1300 - 2100	30 - 112	81	Glasgow-Liv.-Sheff. 79 [18]
11	T	1300 - 2100	30 - 112	81	Glasgow-Liv.-Sheff. 79 [18]
12	G	1300 - 2300	48 - 82	59	Glasgow-Liv.-Sheff. 79 [21]
13	H	1300 - 2300	48 - 82	59	Glasgow-Liv.-Sheff. 79 [21]
14	Ox	450	105	1	Kharkov 79 [22]
15	Oz	450	105	1	Kharkov 79 [22]

1-4. Proton target $\gamma p \to \pi^+ n$, $\pi^0 p$

Data collection for the proton target is satisfactory and nearly completed at low energies $E_\gamma \leq 1$ GeV. The 3rd and the 4th resonance regions are covered by new data from Daresbury [5,11,18,21], but in relatively large steps. In performing analysis, the lack of enough $d\sigma/d\Omega$ data on $\gamma p \to \pi^+ n$ process at energies above 1.4 GeV is a very serious problem. I would like to ask Bonn and Yerevan Institutes to supply these data in the near future. In addition, the role played by the Daresbury data is so important in analyzing the 4th resonance region that the data should be reconfirmed at the operating institutes.

1-5. Neutron target $\gamma n \to \pi^- p$

This process is necessary for the isospin decomposition of resonance amplitudes, but the experiment is extremely difficult due to the Fermi motion of neutrons in the deuteron used as the target. New experimental data published after the DESY Symposium are listed in Table 1c.

The systematic T data from Nagoya-Osaka group [26] well cover the second resonance region. However as is clear from the data map in Fig. 2c, Σ-data are scanty at $E_\gamma > 0.85$ GeV and P-data are even poorer at all energies. At high energies, there is no systematic data for all the observables, and this makes the errors in the neutron coupling determination worse than that for the proton target.

Table 1c. New data ($\gamma n \to \pi^- p$) since 1978

	Obs.	E_γ (MeV)	θ_{cm}	No. of data points	Institute
1	$d\sigma/d\Omega$	231 - 446	90	16	Saclay 78 [23]
2	$d\sigma/d\Omega$	900 - 1650	30 - 60	12	Yerevan 79 [24]
3	P	718 - 1086	60 - 100	19	INS(Tokyo) 80 [25]
4	Σ	900 - 1650	30 - 60	12	Yerevan 79 [24]
5	T	563 - 900	50 - 122	60	Nagoya-Osaka 80 [26]

1-6. Eta photoproduction $\gamma p \to \eta p$

New cross section data (15 data points) on $\gamma p \to \eta p$ measured with the tagged photon technique is presented to this Symposium by Tokyo(INS) group [27]. The data cover an energy range from 0.8 to 1.0 GeV at angles from 45° to 114° (Fig. 3). They analyzed their data together with all existing η photoproduction data(150 data points for $d\sigma/d\Omega$, 8 for P) adopting the Walker's model for 8 resonance contributions with smooth background. Resulting photocouplings for P11(1470) $A_{1/2}$ and S11(1535) $A_{1/2}$ amplitudes are $3 \cdot 10^{-3}$ and $146 \cdot 10^{-3}$ $(\mathrm{GeV/c})^{1/2}$ respectively, and they are consistent with the $\gamma N \to \pi N$ analyses. Here, A represents the helicity 1/2 amplitude. Fitted curves from this analysis are also shown in Fig. 3.

2. Recent phenomenological analysis

Since Walker [28] presented his simple isobar model in 1969, a number of similar analyses were performed adding new data. The original work was revised in 1974 Metcalf-Walker (MW) [29], and the most recent analysis was carried out in 1976 and 1977 by Nagoya group [30] for the proton target by including their own data. This type of analysis is still useful in constructing the imaginary part of partial wave amplitude as a starting solution for a dispersion analysis in the 3rd and 4th resonance region.

Various analyses based on the fixed-t dispersion relation were reported by Devenish-Lyth-Rankin (1974) [31], Moorhouse-Oberlack-Rosenfeld (MOR 1974) [32], Knies-Moorhouse-Oberlack-Rittenberg-Rosenfeld (KMORR 1974) [33], Crawford

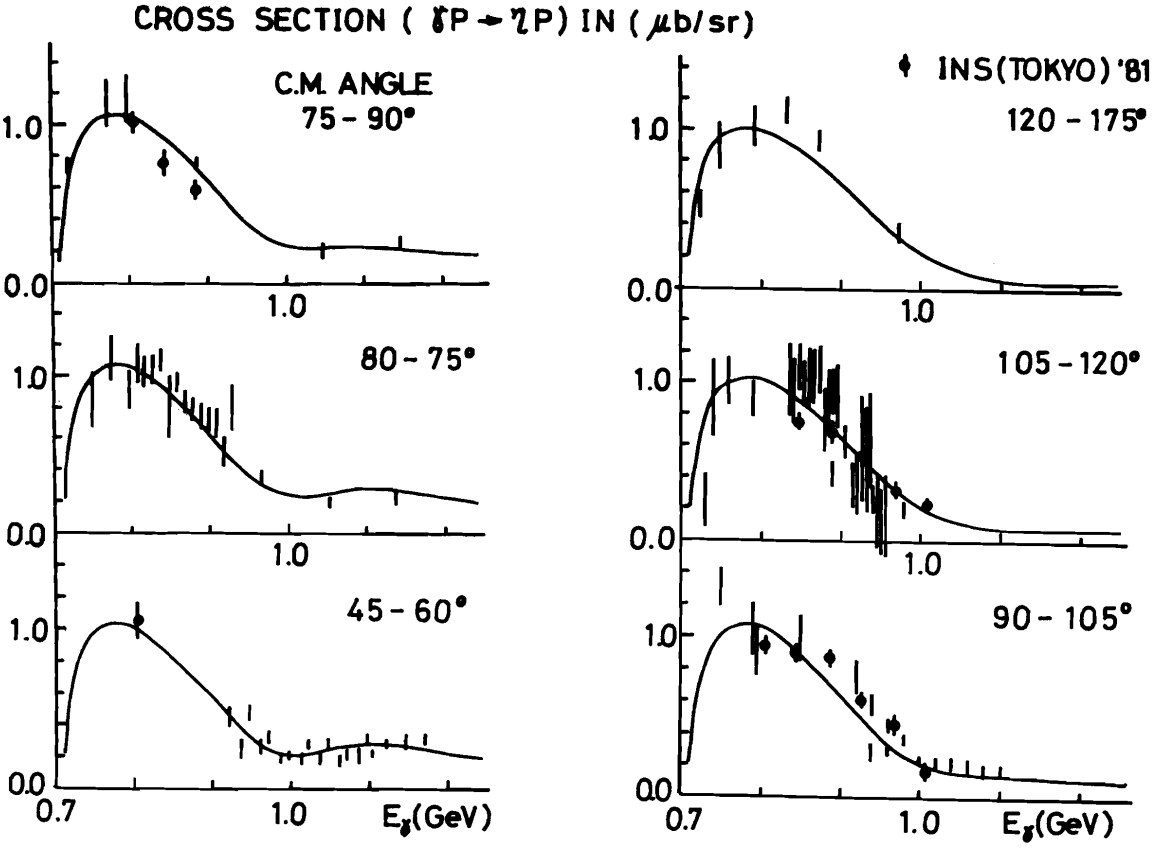

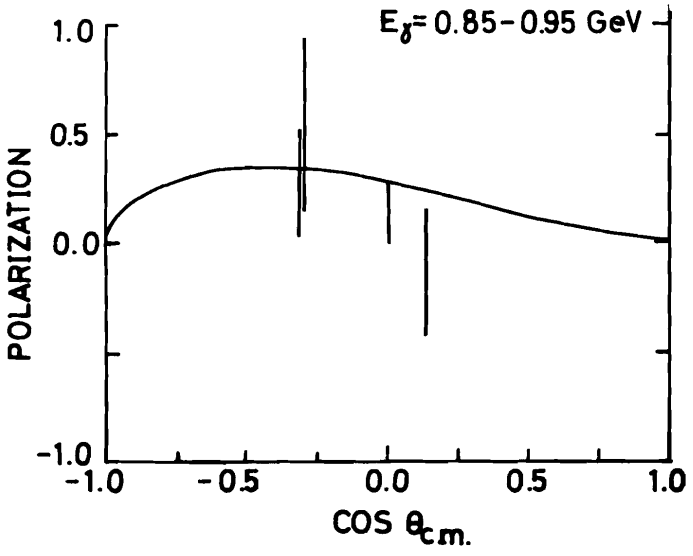

Fig. 3. New $\gamma p \to \eta^0 p$ cross-section data( ) from INS(Tokyo) [27] shown with the existing ones. The solid line represents the result of an isobar analysis done by INS group. The figure below shows recoil proton polarization data fitted by INS analysis. For origins of the other data see Ref.[27].

(C 1975) [34], Barbour-Crawford (BC 1976) [35], Barbour-Crawford-Parsons (BCP 1978) [36], Arai-Fujii (Tokyo 1979) [37] and most recently BCP revised their analysis adding new data in 1980. Noelle (1977) [38] presented a coupled channel analysis considering the multi-channel unitarity and called attention to the existence of resonance-like structures in the background amplitudes. In this Symposium, a new analysis adopting the Tokyo 79 model [37] is reported by Nagoya group (Nagoya 81) [39].

The number of data points used in various analyses are plotted in Fig. 4. Apparently the number of useful data points increased linearly with time, and consequently the experimental photocouplings become more and more accurate.

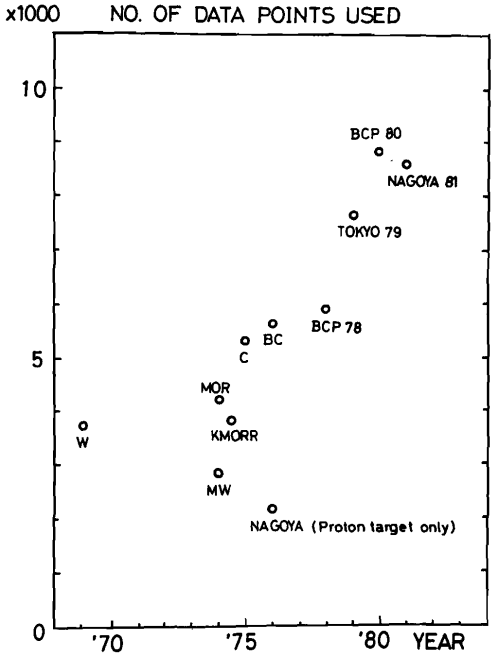

Fig. 4 The number of data points used in various analyses against the year.

2-1. Glasgow analysis (BCP 80)

The first BCP 78 analysis was revised in 1980 adding new data [40]. This analysis uses Walker type amplitudes for the imaginary part of partial wave amplitude, i.e. the resonances are parametrized in Breit-Wigner forms and smooth backgrounds are added. The resonance masses are allowed to deviate from those determined by the πN phase shift analysis. The analyticity is fulfilled through the dispersion relation, and the real and imaginary amplitudes at low energies are mutually related in terms of πN elastic phase shifts by the Watson's theorem. Different parametrizations are applied for the three energy regions, i.e. (a) resonance region (E<2 GeV) (b) Regge region (E>2.5 GeV) and (c) intermediate region (2<E<2.5 GeV) where a special hybrid formula is used to link (a) and (b). The analysis successfully fitted the data up to 16 GeV, obtaining a good χ^2/N value. Errors in photocouplings are determined by considering estimated systematic errors in the experimental data.

2-2. Nagoya 81 analysis

This analysis [39] revised Tokyo 79 by using a new set of resonance parameters given by CMU-LBL group [41] obtained from the πN phase-shift analysis and by removing artificial background terms. Only the resonance mass of D13(1520) is lowered by 20 MeV for a better fit to $d\sigma/d\Omega$. The amplitudes are treated differently depending on the energy, i.e. (a) resonance region (E≤2.2 GeV),

adopting K-matrix formalism with the couplings parametrized in 3 channels (γN, πN and inelastic), (b) Regge region ($E \leq 2.2$ GeV) using the dual absorptive model. The background amplitudes are parametrized in the pseudo-resonance form. The errors assigned to the resulting photocouplings include uncertainties in the πN resonance widths. The results of BCP 80 and Nagoya 81 are tabulated in Table 2a and b for the proton and neutron respectively. The agreement between the two analyses are generally good, except for D13(1700) $A_{3/2}$, P13(1800) $A_{1/2}$ for the proton target, and S11(1650) $A_{1/2}$, D13(1700) $A_{1/2}$, $A_{3/2}$ and P13(1800) $A_{3/2}$ for the neutron target.

2-3. Comparison with the new data

The results of Nagoya 81 analysis are compared with new data in Fig. 5. For comparison, curves from Tokyo 79 analysis are also plotted. In Tokyo 79 analysis, πN phase shift data from Saclay 74 [42] were refitted to determine the strong decay parameters of the resonances.

The new analyses are better as seen, for example, in the comparison with the latest $d\sigma/d\Omega$ ($\gamma p \to \pi^+ n$) data [3] from Bonn (Fig. 5a). Improved fits are particularly noted at large angles and at high energies ($E \geq 1$ GeV). This clearly shows the consideration of higher mass resonances with proper parametrizations are essential for the accurate determination of couplings at the energies higher than 1 GeV.

From BCP 80 and Nagoya 81 analyses, the photocouplings are determined up to the 3rd resonance region ($M \leq 1.7$ GeV) for proton target and up to the 2nd resonance ($M \leq 1.5$ GeV) for neutron target, and the errors of neutron couplings in the 3rd resonance region are appreciably reduced (exceptions: S11(1650) and D13(1700)). Two resonances in the 4th resonance region, F35(1910) and F37(1950), are also well determined by the new analyses.

3. Comparison with quark model

3-1. Quark models

Recently, QCD inspired quark models were presented by Ohta (1979) [43], Barbour-Ponting (BP 1980) [44] and Koniuk-Isgur (KI 1980) [45], and they succeeded to give correct signs to all the photocouplings including P11(1470) "Roper" resonance. In these models, the spin-orbit force in the 3-body quark-quark interaction are cancelled or neglected adopting the Isgur-Karl model [46]. The true meaning of the cancellation of spin-orbit force was debated in the Baryon Conference in 1980, however we have no conclusive agreement so far. More studies of the quark model with a quantitative comparison with the experimental evidences are therefore required.

In this year, Forsyth (1981) [47] presented a tentative quark model in which he tried to determine theoretical parameters in the model from the fit to experimental data, i.e. resonance masses, strong decays and photocouplings. The results are; (1) QCD motivated quark shell models are good, (2) the decoupling of many resonances from the πN channel predicted by IK 80 model [46] is confirmed, and the same is true also for the odd-parity states, (3) non-spectator model fits the data best, (4) contact force (spin-spin) parameter varies from band to band in [SU(6)×O(3)] super multiplets [5], no positive evidence has been found for a tensor force, while conflicting evidence has been found for a three body spin-orbit force. For further developments, more reliable data are required for P-waves in 1.4-1.7 GeV, and also 1.9-3.0 GeV data are highly desirable in order to observe N=3 band structure.

In Table 2a and b, I listed the experimental photocouplings and the corresponding quark model predictions given by KO, IK, BP and Forsyth for comparison. The agreement between the theories are fair. Two models, IK and Forsyth, are most successful when compared to BCP 80 and Nagoya 81. However, the qualification of the theories is far from being excellent.

3-2. Summary of photocoupling determination

(1) Accuracy in photocoupling determination substantially increased as data maps were filled more densely. The agreement between recent analyses is good for resonance $M \leq 1.7$ GeV.
(2) More accurate πN resonance parameters are necessary for the determination of high-mass resonance couplings ($M > 2$ GeV).
(3) More photoproduction data at higher energies are required; particularly waited are

Table 2a. Radiative Decay Matrix Elements off Proton (unit: 10^{-3} $GeV^{-1/2}$)

Multiplet	Resonance	Amplitude	Analysis				Quark Model		
			Glasgow	Tokyo	Nagoya 81	Forsyth	KI	BP	KO
[56,0+]0	P33(1232)	$A_{1/2}$	-136 ± 6	-147 ± 1	-138 ± 4	-127	-103	-94	-101
		$A_{3/2}$	-247 ± 10	-264 ± 2	-259 ± 6	-220	-179	-162	-176
[56,0+]2	P11(1470)	$A_{1/2}$	-68 ± 15	-69 ± 4	-63 ± 8	-50	-20	-24	-5
	P33(1600)	$A_{1/2}$	5 ± 20		-46 ± 13	-50	-16		
		$A_{3/2}$	-9 ± 20		25 ± 31	-87	-46		
[70,1-]1	S11(1535)	$A_{1/2}$	65 ± 16	83 ± 7	77 ± 21	68	147	95	84
	S11(1650)	$A_{1/2}$	31 ± 17	65 ± 5	50 ± 10	-9	88	95	49
	D13(1520)	$A_{1/2}$	-19 ± 7	-32 ± 5	-7 ± 4	-41	-23	-28	6
		$A_{3/2}$	167 ± 10	178 ± 3	168 ± 13	161	128	95	171
	D13(1700)	$A_{1/2}$	-24 ± 19	-28 ± 7	-2 ± 13	-3	-7	9	-1
		$A_{3/2}$	-17 ± 14	-2 ± 5	29 ± 14	33	11	-12	-33
	D15(1670)	$A_{1/2}$	23 ± 15	6 ± 5	34 ± 5	9	12	0	0
		$A_{3/2}$	3 ± 12	30 ± 4	24 ± 8	12	16	0	0
	S31(1650)	$A_{1/2}$	21 ± 20	-22 ± 7	10 ± 15	74	59	43	86
	D33(1670)	$A_{1/2}$	125 ± 22	112 ± 6	89 ± 33	106	100	78	90
		$A_{3/2}$	102 ± 15	47 ± 7	60 ± 15	79	105	78	91
[70,0+]2	P11(1710)	$A_{1/2}$	15 ± 25	-9 ± 6	28 ± 9	-37	-24		-7
[56,2+]2	F15(1690)	$A_{1/2}$	-18 ± 14	-28 ± 9	-9 ± 6	6	0	-7	24
		$A_{3/2}$	141 ± 14	115 ± 8	115 ± 8	154	91	47	106
	P13(1800)	$A_{1/2}$	38 ± 50	51 ± 25	-4 ± 7	36	46	74	42
		$A_{3/2}$	-14 ± 40	-58 ± 26	-40 ± 16	-65	-133	-23	-54
	P31(1900)	$A_{1/2}$	13 ± ?	-12 ± 12	25 ± 11	5	0	15	-16
	F35(1890)	$A_{1/2}$	24 ± 14	22 ± 26	43 ± 20	44	-33	-10	20
		$A_{3/2}$	-72 ± 35	-29 ± 18	-25 ± 23	15	8	-41	-8
	F37(1950)	$A_{1/2}$	-67 ± 14	-91 ± 12	-68 ± 7	-48	-69	-25	-34
		$A_{3/2}$	82 ± 17	-101 ± 14	-94 ± 16	-61	-50	-32	-44
	P33(1920)	$A_{1/2}$			40 ± 14	-22			
		$A_{3/2}$			23 ± 17	38			

Table 2a.(continued) Radiative Decay Matrix Elements off Proton (unit: 10^{-3} $GeV^{-1/2}$)

			Analysis				Quark Model		
Multiplet	Resonance	Amplitude	Glasgow	Tokyo	Nagoya 81	Forsyth	KI	BP	KO
[70,2+]2	F17(1970)	$A_{1/2}$	1 ± 40		30 ± 29	-10	-8		
		$A_{3/2}$	4 ± 25		86 ± 60	-13	-10		
[56,1-]3	D13(1880)	$A_{1/2}$			-20 ± 8	-13			
		$A_{3/2}$			17 ± 11	63			
	S31(1990)	$A_{1/2}$	-6 ∿ -25		29 ± 8	-3			
	D33(1940)	$A_{1/2}$			-36 ± 58	15			
		$A_{3/2}$			-31 ± 12	4			
	D35(1940)	$A_{1/2}$	-38 ± 47		9 ± 9	-17			
		$A_{3/2}$	-28 ± 80		-25 ± 11	-24			

Table 2b. Radiative Decay Matrix Elements off Neutron (unit: 10^{-3} $GeV^{-1/2}$)

			Analysis				Quark Model		
Multiplet	Resonance	Amplitude	Glasgow	Tokyo	Nagoya 81	Forsyth	KI	BP	KO
[56,0+]2	P11(1470)	$A_{1/2}$	56 ± 15	23 ± 9	37 ± 10	38	16	13	4
[70,1-]1	S11(1535)	$A_{1/2}$	-98 ± 26	-75 ± 9	-35 ± 14	-102	-119	-45	-89
	S11(1650)	$A_{1/2}$	-68 ± 40	10 ± 20	-8 ± 4	-6	-35	-45	-48
	D13(1520)	$A_{1/2}$	-56 ± 11	-76 ± 6	-66 ± 13	-23	-45	-29	-48
		$A_{3/2}$	-144 ± 15	-147 ± 8	-124 ± 9	-124	-122	-102	-144
	D13(1700)	$A_{1/2}$	52 ± 35	-52 ± 30	6 ± 24	23	-15	-9	25
		$A_{3/2}$	41 ± 30	-37 ± 36	-33 ± 17	-28	-76	-42	-38
	D15(1670)	$A_{1/2}$	-59 ± 15	-39 ± 17	-57 ± 24	-55	-37	-31	-36
		$A_{3/2}$	-59 ± 20	-66 ± 26	-77 ± 18	-78	-53	-44	-51
[70,0+]2	P11(1710)	$A_{1/2}$	-17 ± 20	11 ± 21	0 ± 18	29	-21		2
[56,2+]2	P13(1800)	$A_{1/2}$	-3 ± 34	-19 ± 87	2 ± 5	12	-10	-23	13
		$A_{3/2}$	18 ± 28	-139 ± 105	-15 ± 19	-61	57	0	12
	F15(1690)	$A_{1/2}$	44 ± 12	26 ± 5	17 ± 14	-32	26	27	19
		$A_{3/2}$	-33 ± 15	-24 ± 9	-33 ± 13	2	-25	0	-21
[70,2+]2	F17(1970)	$A_{1/2}$	-78 ± 30		-1 ± ?	-19	-18		
		$A_{3/2}$	-116 ± 45		-178 ± ?	-25	-23		
[56,1-]3	D13(1880)	$A_{1/2}$			7 ± 13	4			
		$A_{3/2}$			-53 ± 34	-34			

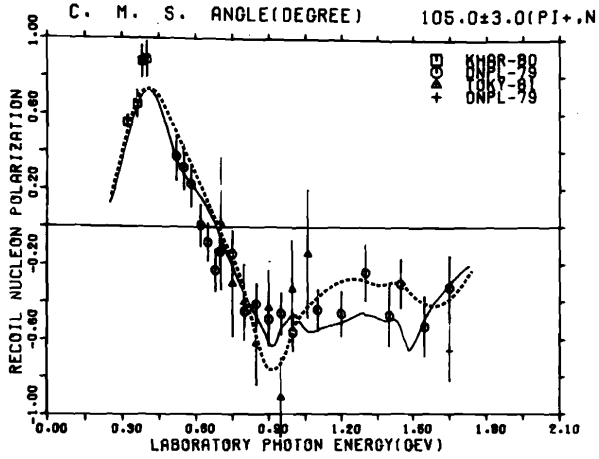

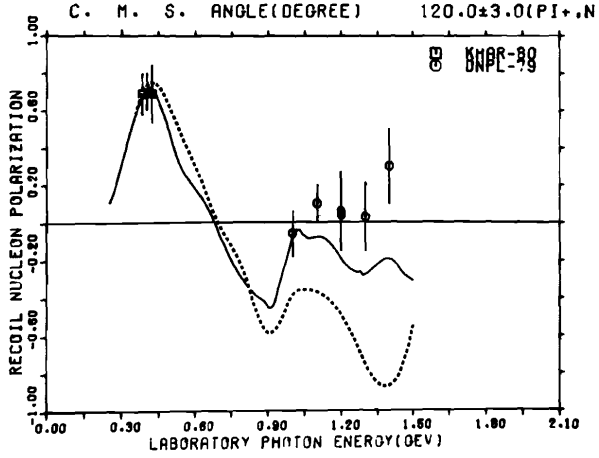

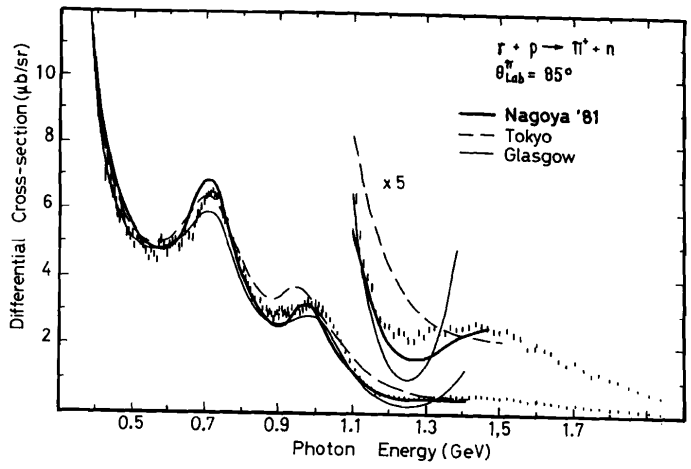

Fig. 5a. New $\gamma p \to \pi^+ n$ cross-section data from Bonn [3], compared with recent analyses.

Fig. 5b. New $\gamma p \to \pi^+ n$ recoil nucleon polarization data from Tokyo(TOKY-81)[6], Daresbury(DNPL-79)[5] and Kharkov(KHAR-80)[4]. The solid curve is the prediction by Nagoya-81[39] and the dotted curve by Tokyo[37].

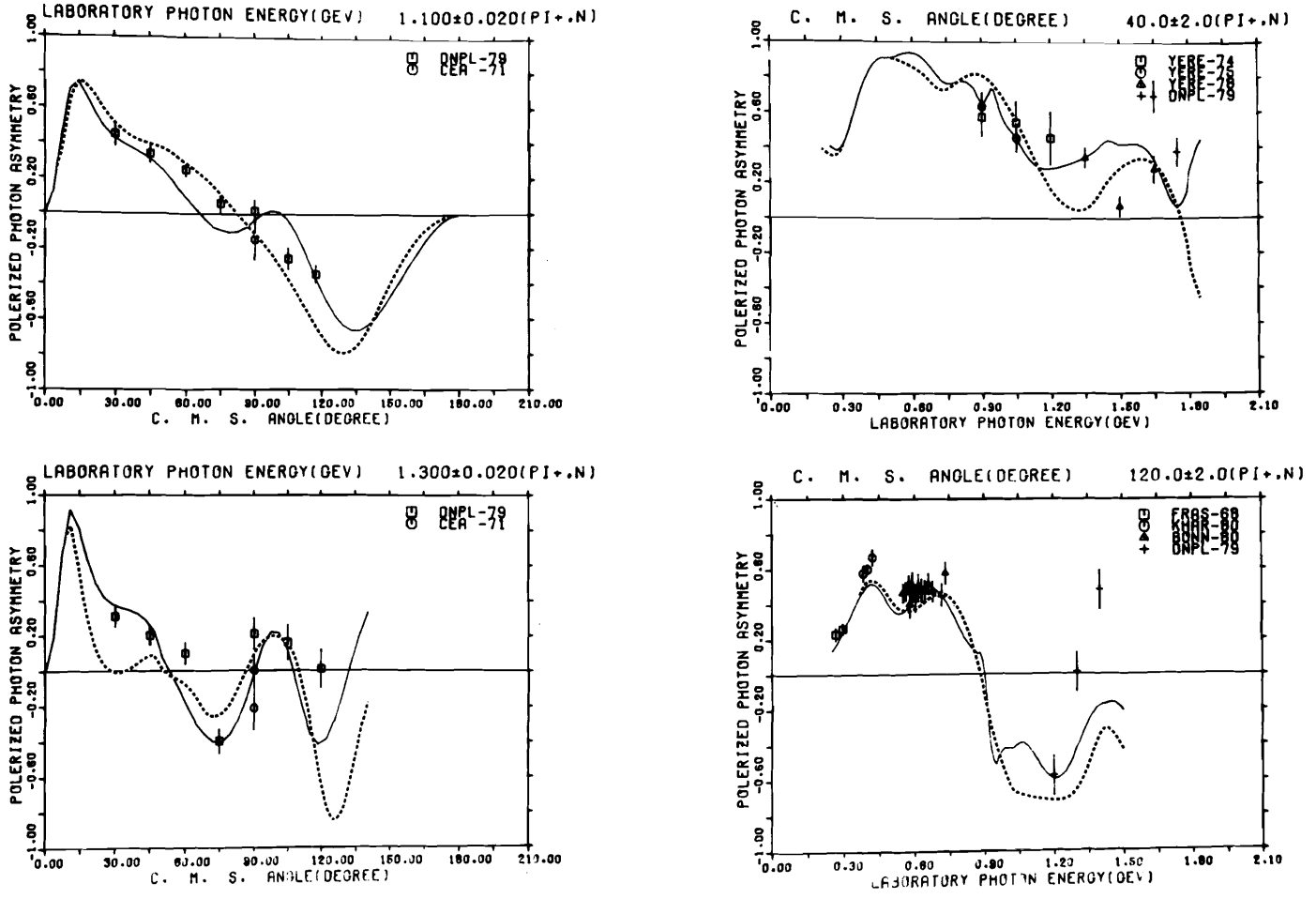

Fig. 5c. New Σ data on $\gamma p \to \pi^+ n$ from Daresbury(DNPL-79)[5], Kharkov(KHAR-80)[4], Bonn(BONN-80)[7] and Yerevan(YERE-78)[8]. The curves are the same as fig. 5b.

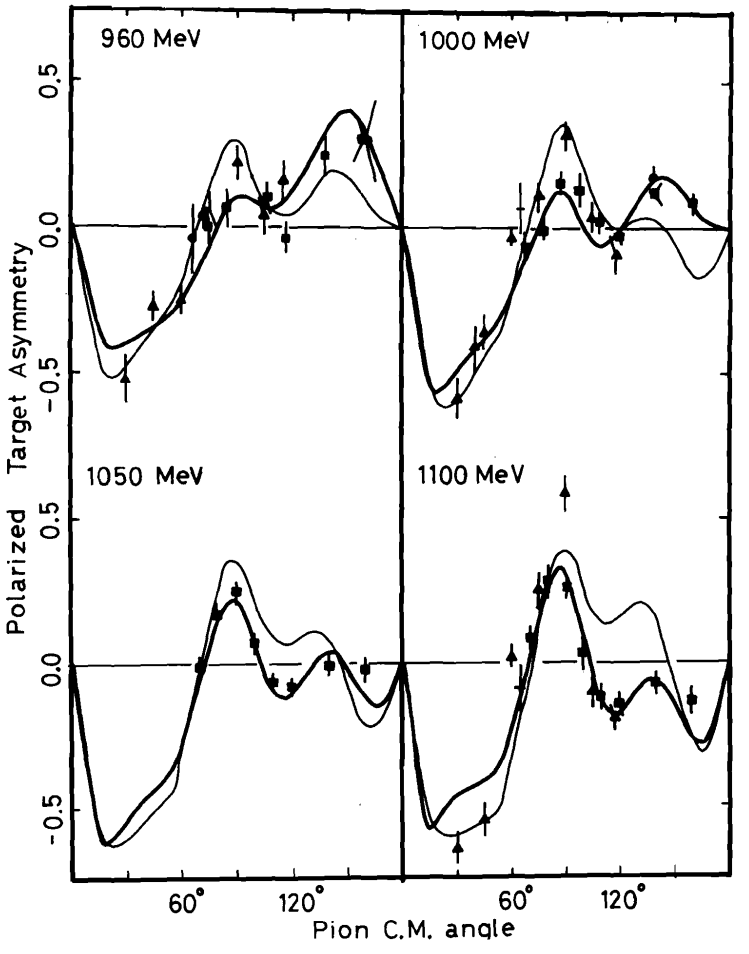

Fig. 5d. New T data on $\gamma p \to \pi^+ n$ from Nagoya(●)[10], plotted together with the data from Bonn(+)[79], Daresbury(▲)[5] and previous Nagoya(◆)[80]. The thick curve is the fit by Nagoya-81[39] and the thin curve by Tokyo[37].

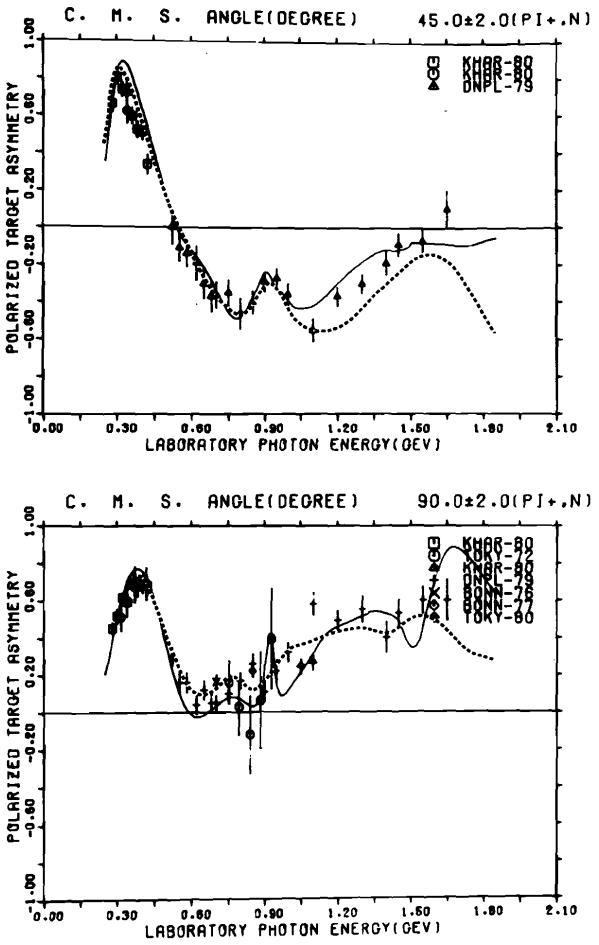

Fig. 5e. New T data on $\gamma p \to \pi^+ n$ from Nagoya (TOKY-81)[15], Daresbury(DNPL-79)[5] and Kharkov(KHAR-80)[4,9]. Other data are taken from Ref.[81]. The curves are the same as in fig. 5b.

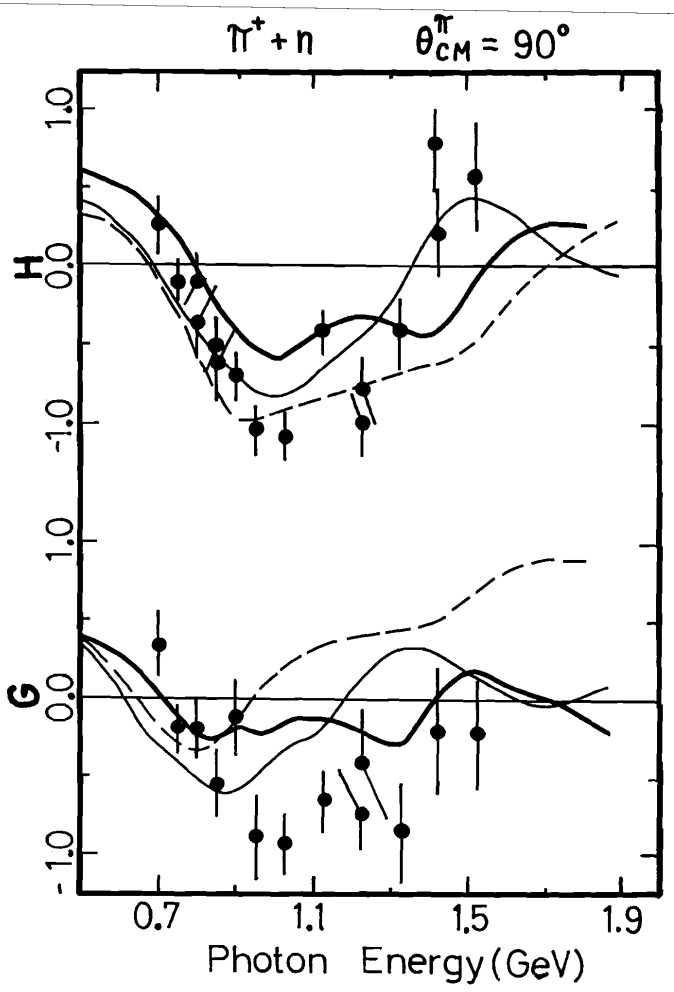

Fig. 5f. First data on the double polarization observables, G and H, for $\gamma p \to \pi^+ n$ from Daresbury [11]. The thick curve is the prediction by Nagoya-81[39], the dotted curve by Tokyo[37] and the thin curve by Glasgow[36].

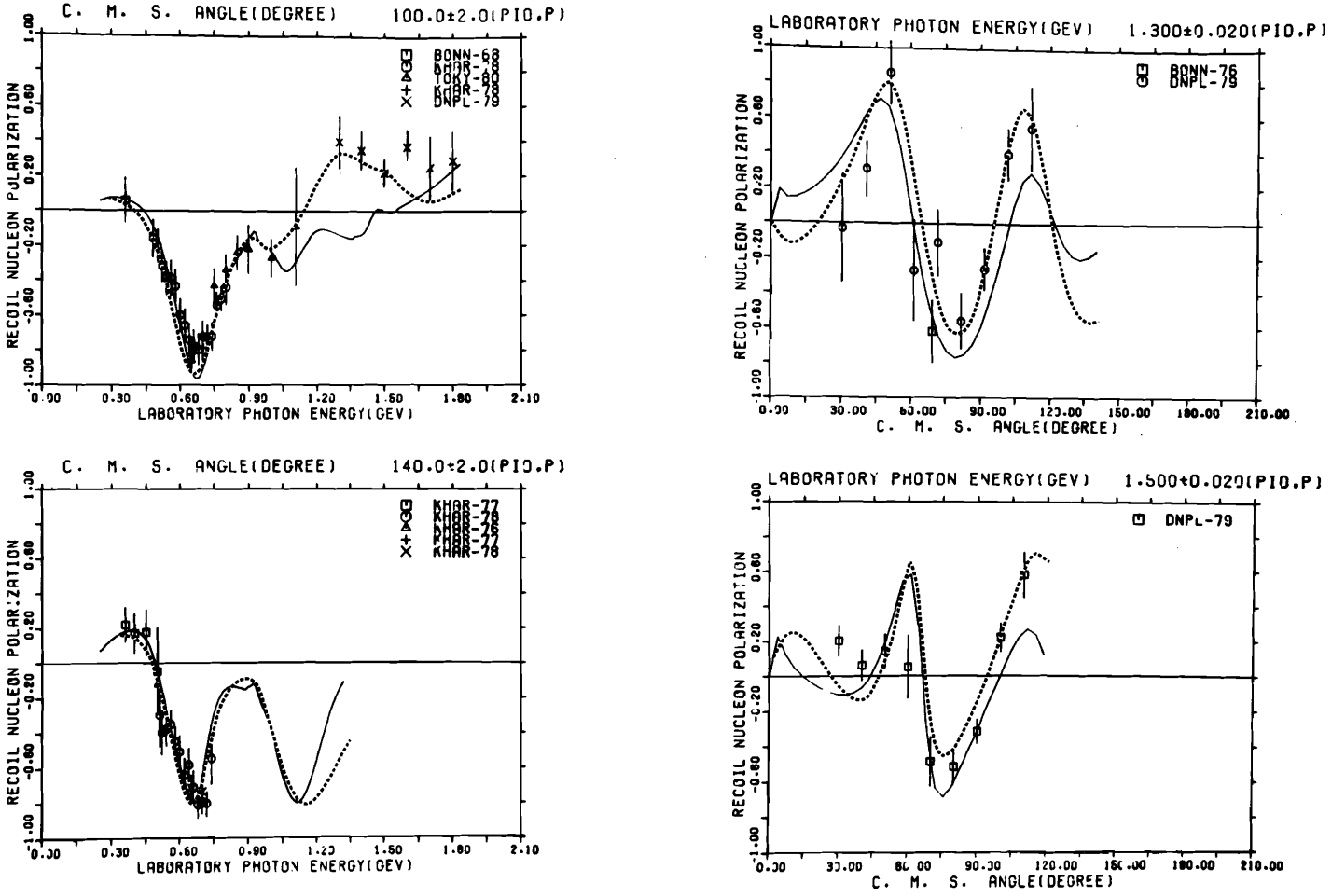

Fig. 5g. New P data on $\gamma p \to \pi^0 p$ from Tokyo(TOKY-80)[17] and Daresbury(DNPL-79)[18] are compared with the previous data (Ref.[81]) and recent analyses (see the caption of fig. 5b.).

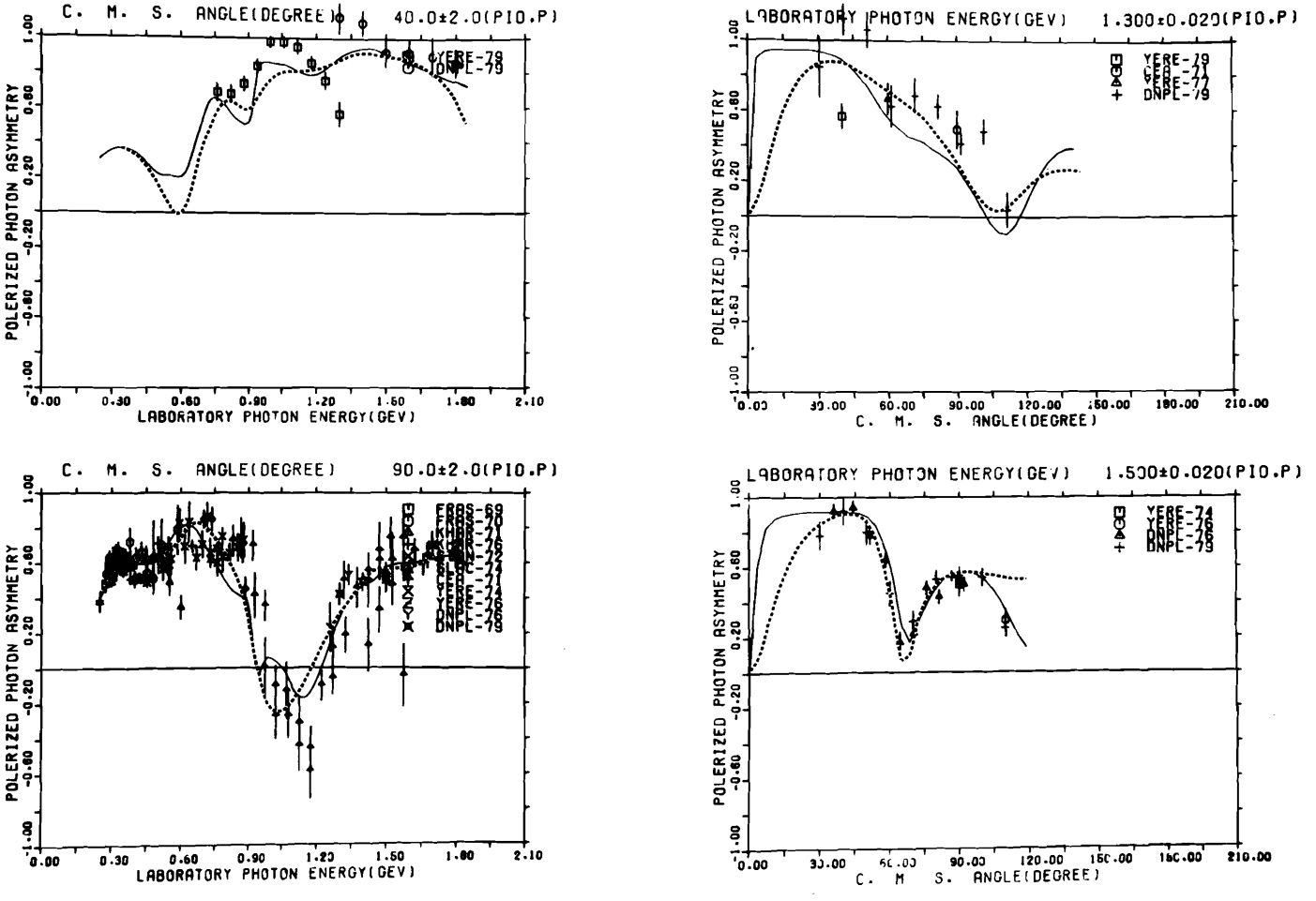

Fig. 5h. New Σ data on $\gamma p \to \pi^0 p$ from Yerevan(YERE-79)[20] and Daresbury(DNPL-79)[18]. See the caption of fig. 5b for the curves and Ref.[81] for other data.

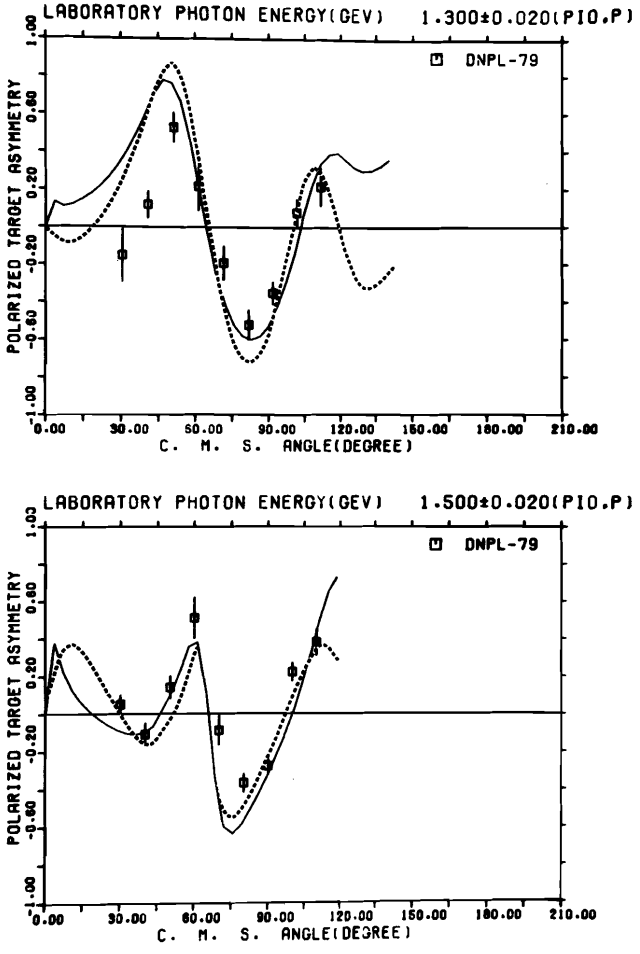

Fig. 5i. New T data on $\gamma p \to \pi^0 p$ from Daresbury [18] compared with the recent analyses (see the caption of fig. 5b.)

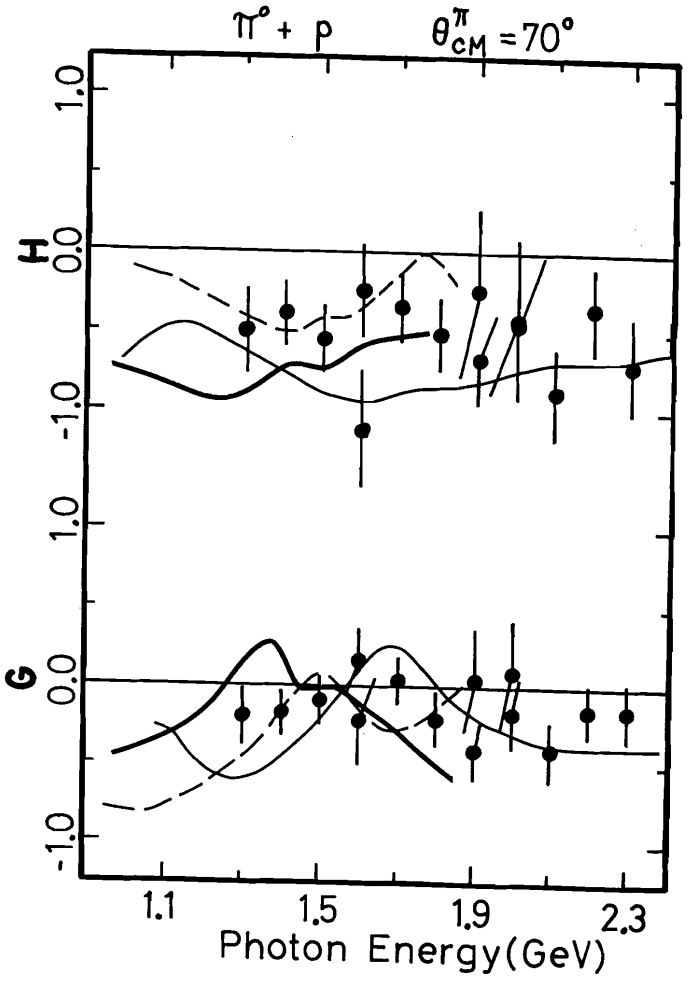

Fig. 5j. First data on the double polarization observables, G and H, for $\gamma p \to \pi^0 p$ from Daresbury [21]. The curves are the same as fig. 5f.

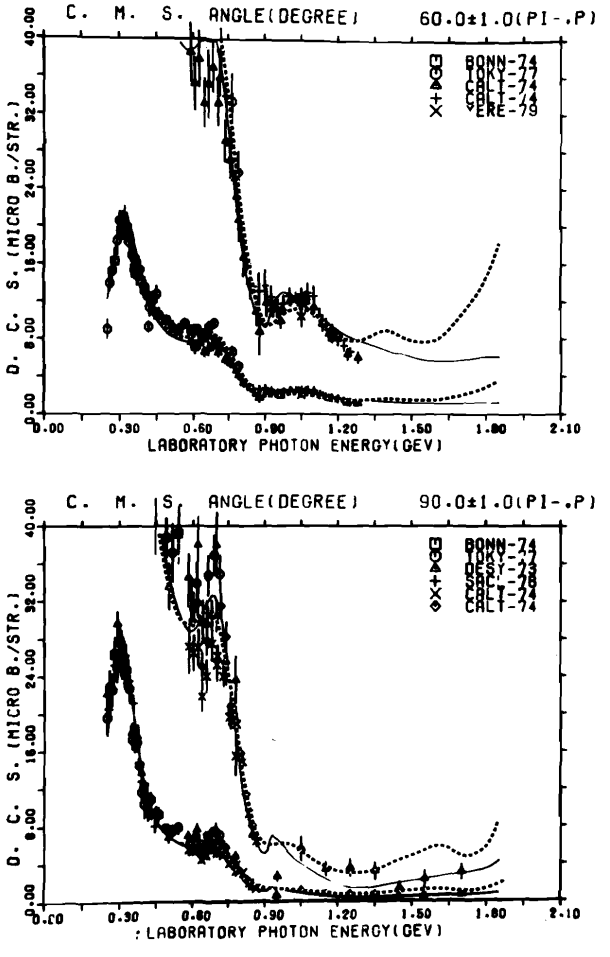

Fig. 5k. New data on $d\sigma/d\Omega$ for $\gamma n \to \pi^- p$ from Saclay(SACL-78)[23] and Yerevan(YERE-79)[24]. See the caption of fig. 5b. for the curves and Ref.[81] for other data.

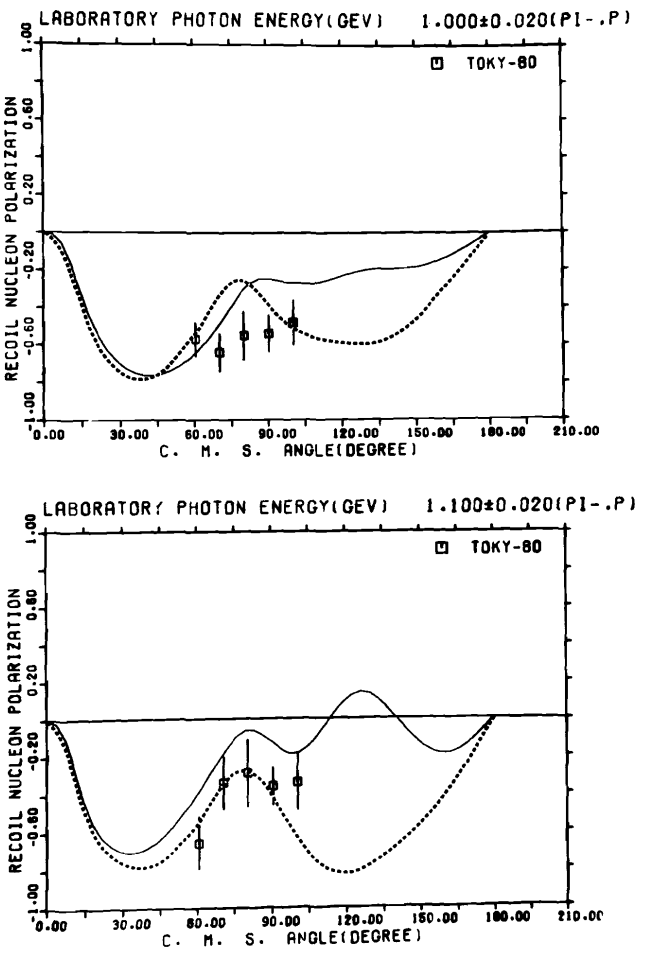

Fig. 51. New P data on $\gamma n \to \pi^- p$ from Tokyo (TOKY-80)[25]. The curves are the same as fig. 5b.

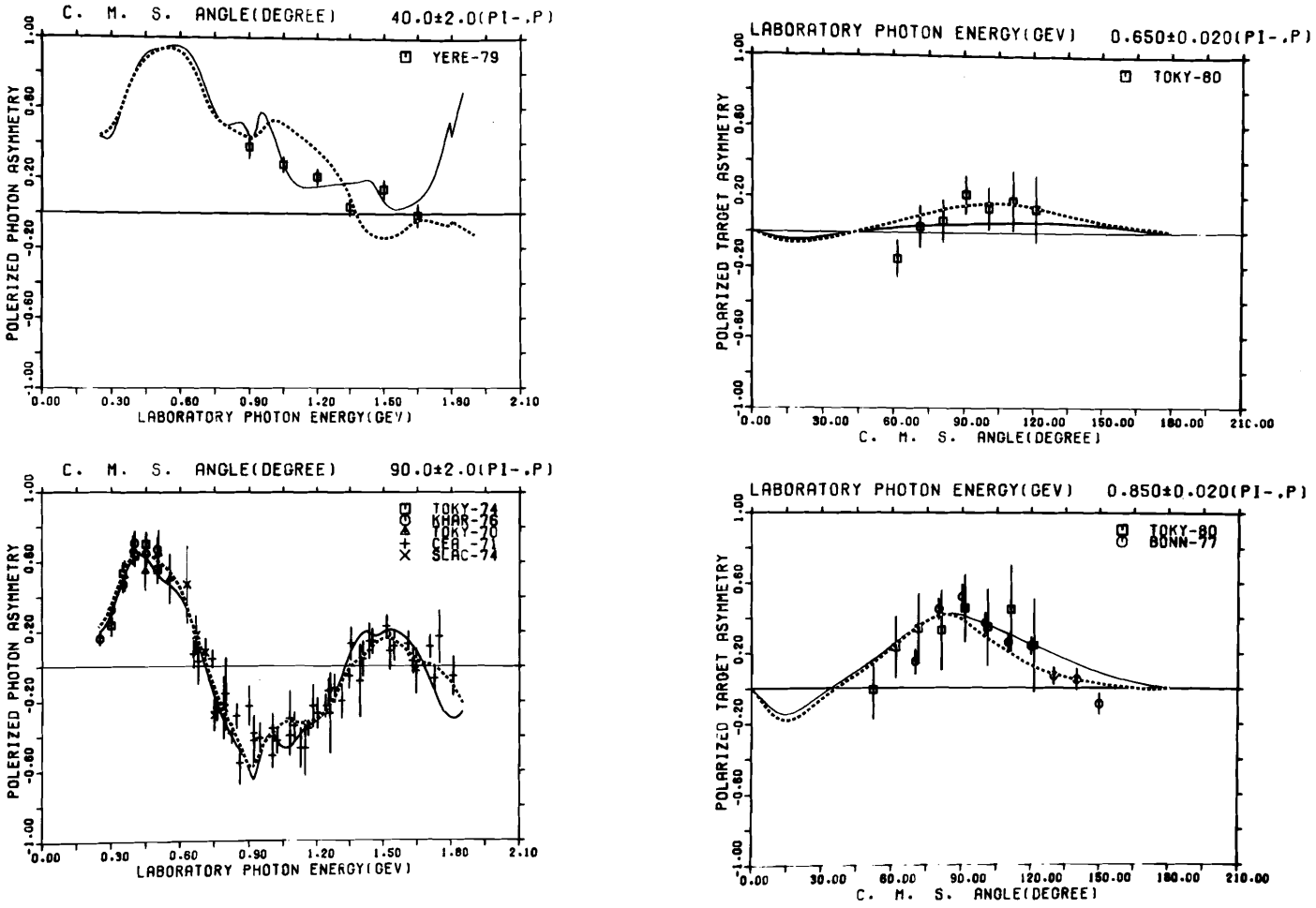

Fig. 5m. New $\gamma n \to \pi^- p$ data from Yerevan(YERE-79)[24] for Σ and Nagoya(TOKY-80)[26] for T. See the caption of fig. 5b. for the curves and Ref.[81] for other data.

- $d\sigma/d\Omega$ ($\gamma p \to \pi^+ n$) data,
- confirmation of Daresbury D.P.M. data,
- neutron target experiments for all observables.

(4) Predictions by QCD inspired quark models agree fairly well with experiments.
(5) Quantitative comparison with improved quark model will offer knowledges on the quark 3-body force, i.e. the spin-orbit force and the band structure of [SU(6)×O(3)] multiplets etc.
(6) The recommended photocoupling 1981 is as follows:

Resonance	Amplitude	Proton target	Neutron target
P33(1232)	$A_{1/2}$	-140	-
	$A_{3/2}$	-260	-
P11(1470)	$A_{1/2}$	-60	40
S11(1535)	$A_{1/2}$	70	poor
S11(1650)	$A_{1/2}$	45	bad
D13(1520)	$A_{1/2}$	-20	-60
	$A_{3/2}$	160	-140
D13(1700)	$A_{1/2}$	$0 \sim -20$	bad
	$A_{3/2}$	poor	bad
D15(1670)	$A_{1/2}$	20	-50
	$A_{3/2}$	10	poor
S31(1650)	$A_{1/2}$	10	-
D33(1670)	$A_{1/2}$	100	-
	$A_{3/2}$	90	-
P11(1710)	$A_{1/2}$	20	poor
F15(1690)	$A_{1/2}$	-10	poor
	$A_{3/2}$	130	-20
P31(1900)	$A_{1/2}$	10	-
F35(1890)	$A_{1/2}$	20	-
	$A_{3/2}$	-70	-
F37(1950)	$A_{1/2}$	-80	-
	$A_{3/2}$	-90	-

4. New data on Compton scattering $\gamma p \to \gamma p$

4-1. New data

New data contributed to this Symposium and those published since 1978 are listed in Table 3. All the available data are mapped in Fig. 6 for $d\sigma/d\Omega$ and the recoil proton polarization P. A systematic set of data presented by Bonn group [48] covers the 2nd resonance region, and hence an extensive analysis for $\gamma p \to \gamma p$ becomes possible. New results on P are presented by INS(Tokyo) group [50] to this Symposium. Though with relatively large statistical errors, these data will play an important role in understanding the scattering mechanism.

Table 3. New data ($\gamma p \to \gamma p$) since 1978

	Obs.	E_γ (MeV)	θ_{cm}	No. of data points	Institute
1	$d\sigma/d\Omega$	692 -1002	35 - 132	80	Bonn 81 [48]
2	$d\sigma/d\Omega$	375 - 1150	70, 100, 130	73	INS(Tokyo) 80 [49]
3	P	406 - 977	100, 134	11	INS(Tokyo) 81 [50]

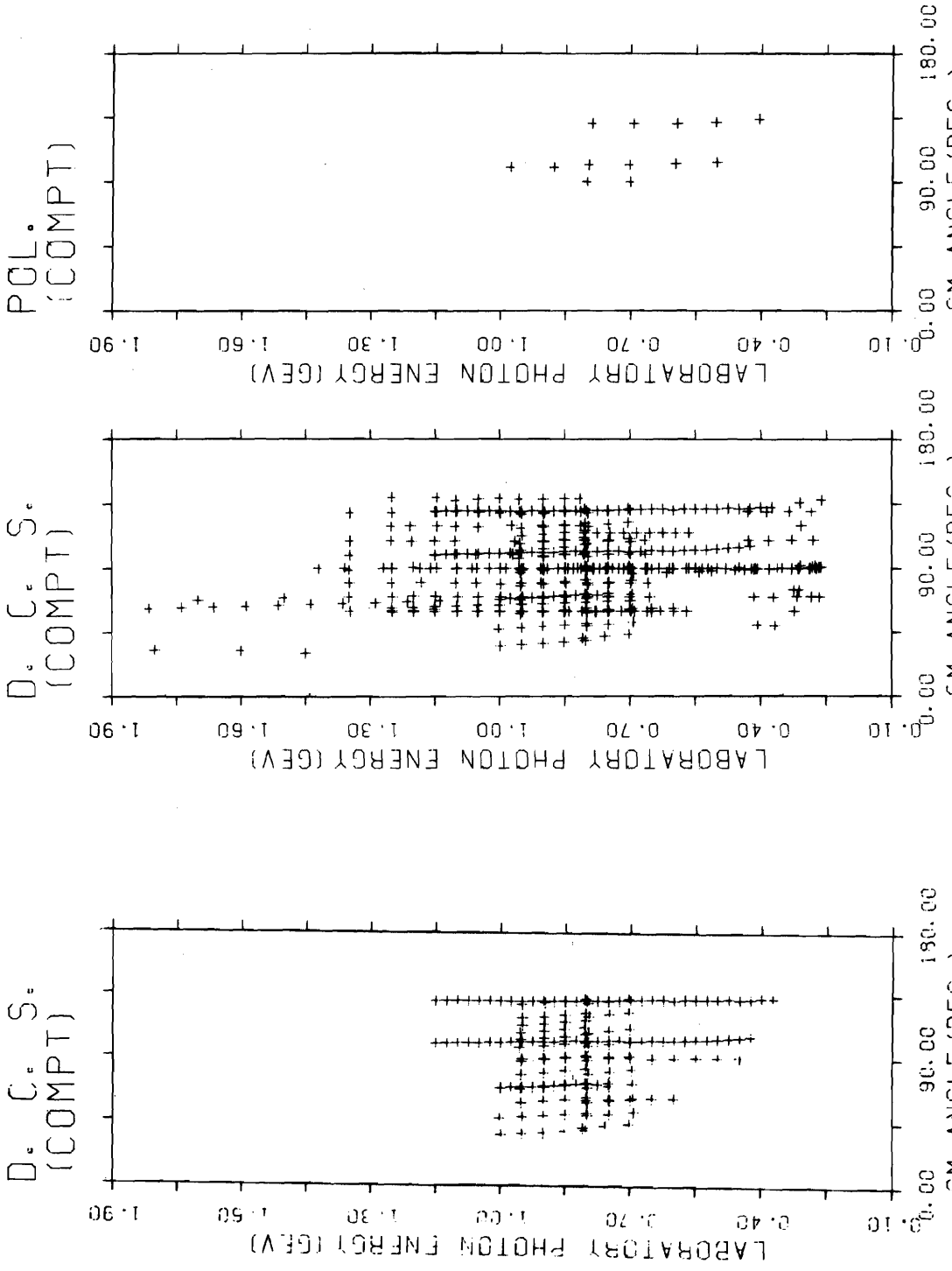

Fig. 6. Data maps 1981 for 2 observables on the proton compton scattering. New data $d\sigma/d\Omega$ after 1978 are also shown for comparison on the left side.

4-2. Dip in the angular distribution

The $d\sigma/dt$ data from Bonn [48] are shown in Fig. 7 for photon energies from 0.7 to 0.95 GeV. The most striking feature of the data is the existence of a sharp dip around $|t| \sim 0.6$ GeV at all energies. The position of the dip shifts linearly from $|t|=0.55$ to 0.72 as the photon energy increases from 0.7 to 0.95 GeV .

The existence of the dip structure in the Compton scattering was first predicted by Harari in 1971 by his dual absorptive model [51], and the prediction is in accordance with the overall behaviour of the measured data. A tentative comparison of the data is made with the averaged contribution of elastic πN scattering data,

$$(\alpha^2/2) \cdot [d\sigma/dt(\pi^+ p) + d\sigma/dt(\pi^- p)]_{\text{elastic}}$$

(α: electromagnetic fine structure constant).

The gross features of the observed angular distribution are well reproduced by the elastic data curve, i.e. a diffractive forward peak, a minimum at $t \sim -0.6$ GeV^2 and a re-rise toward backward angles, as is seen in the 0.8 GeV data (Fig. 7). It is interesting to find a good absolute agreement between the curves and the small angle data. The coupling strength, however, does not agree with the simple ρ-dominance model, being a factor of 2 smaller than the generally accepted value for the γ-ρ coupling.

As suggested by a Legendre polynomial fit to the data, partial waves with j up to 7/2 are required to reproduce such a rapid variation with angle. In order to study the dip structure, Bonn group (Kölbel et al.,) [52] made a dynamical analysis considering partial wave up to j=5/2 for πN, 3/2 for ΔN and 5/2 for other resonances. Their results for the lower bound on the cross section (unitary bound) are shown in Fig. 8 for energies 0.7 and 0.95 GeV together with the $d\sigma/d\Omega$ data. If real parts of scattering amplitudes are small, this bound will reproduce the main features of the data. Theoretical curves are, however, less structured than the observed dip and only the gross parameter is reproduced such as the magnitude of forward-backward asymmetry. It is apparent that we need to include higher waves. A coupled-channel analysis seems highly desirable.

The $d\sigma/d\Omega$ data from INS(Tokyo [47] show no appreciable dip around the c.m. angle of 100° at energies about 0.8 GeV though the data are only at 70, 90, 100 and 130° (Fig. 9). The new P data presented by INS(Tokyo) group [50], at c.m. angles at 100 and 130°, are compared in Fig. 10 with the existing analysis by INS 78 (Toshioka et al.,) [53] which considered the unitarity and dispersion relations.

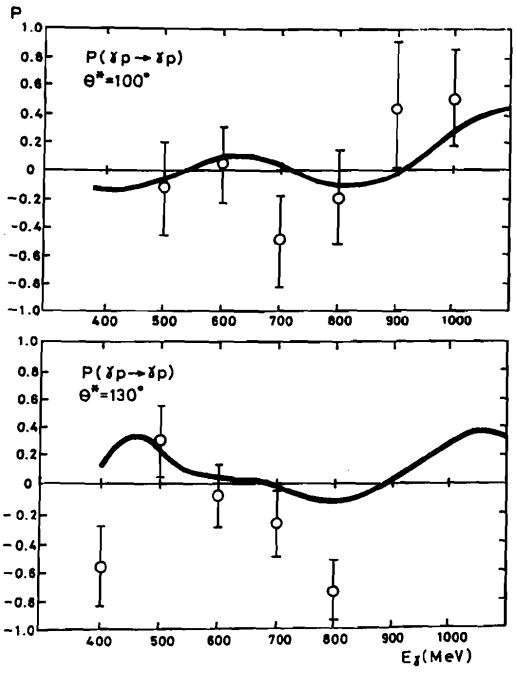

Fig. 10 New recoil proton polarization data for $\gamma p \to \gamma p$ measured by INS(Tokyo) group [50]. The dotted line represents the analysis by INS(Tokyo) [53].

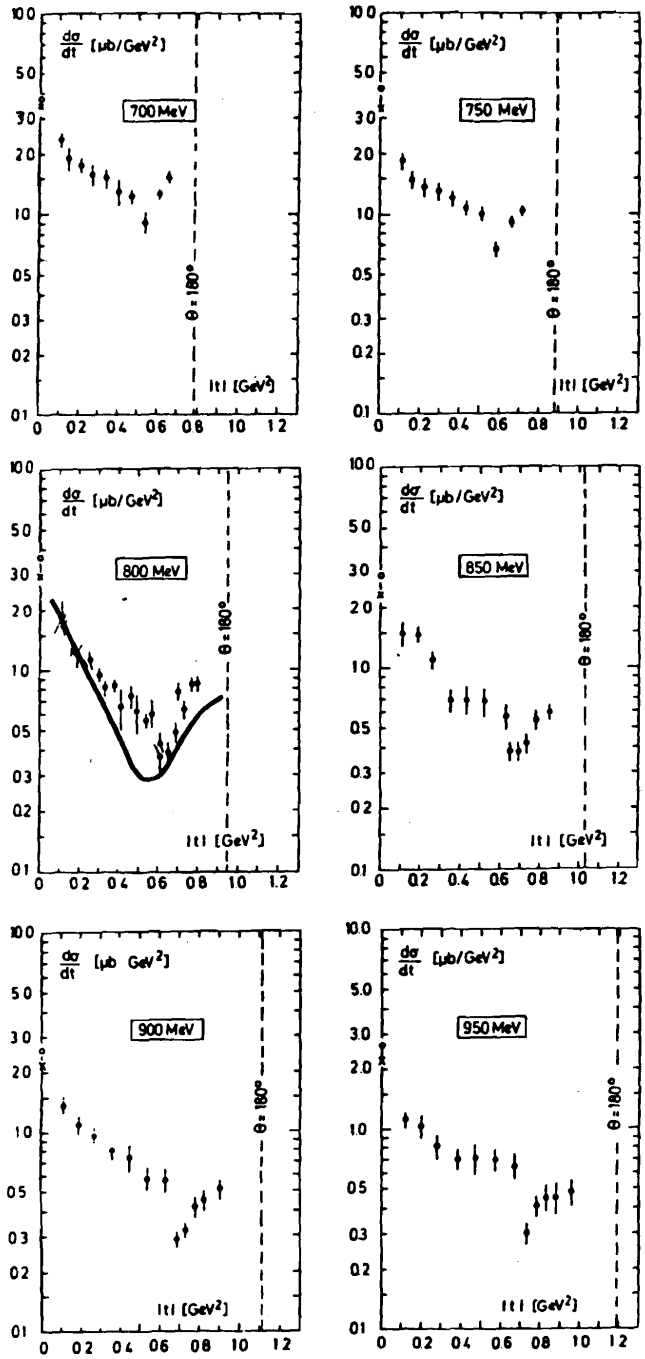

Fig. 7. New differential cross-section data for p p measured by Bonn group[48]. The curve at 800 MeV is the mean value of the elastic π^+p and π^-p scatterings, reduced by a factor α^2.

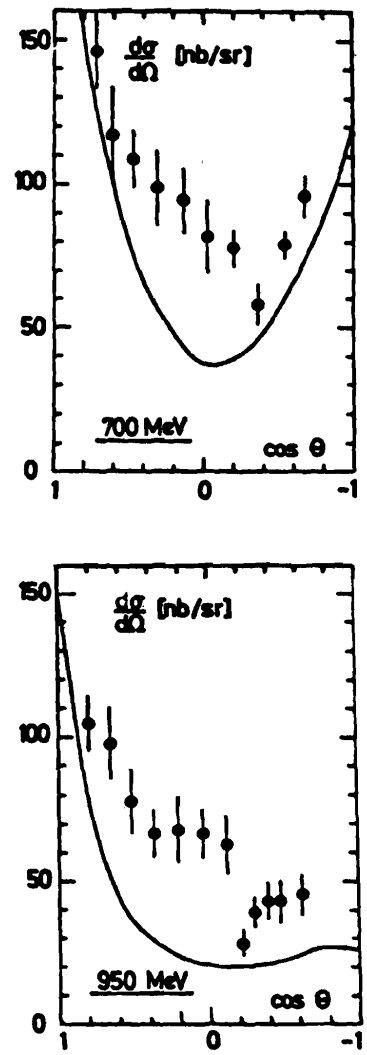

Fig. 8. The Bonn $\gamma p \to \gamma p$ data[48] compared with the unitarity bound of Ref.[52].

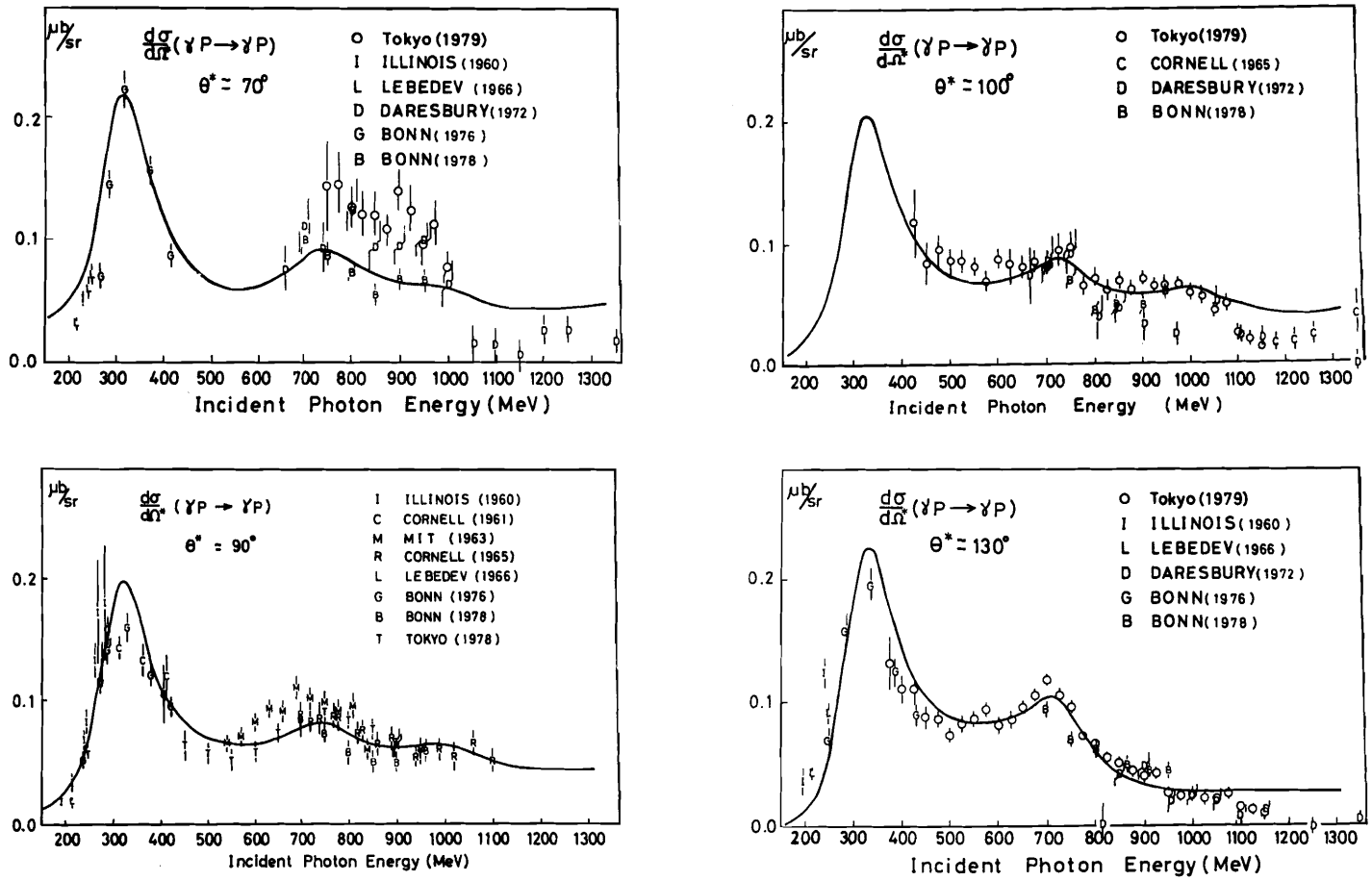

Fig. 9. New cross-section data on γp → γp measured by INS(Tokyo)[49]. The curves are taken from the analysis by INS(Tokyo)[53].

II. γ_v-Coupling of Nucleon Resonance ($Q^2>0$)

The q^2 dependences of nucleon resonance form factors provide more detailed informations about the electromagnetic structure of $[SU(6)\times O(3)]$ supermultiplets than the real-photon couplings do. Experimentally, this new parameter is controlled by varying the virtual photon mass in the meson electroproduction process. The data thus obtained should be confronted with extension of the quark models which were successful in describing the phenomena at $Q^2=0$.

1. New data on electroproduction

In order to perform a reliable multipole analysis, required are a large amount of data measured over wide ranges of the hadron mass W, and the meson production angles θ and ϕ at each Q^2 value. So far, the following processes have been used to determine various multipole couplings,

$\gamma_v p \to \eta p$: S11(1535), D13(1520) for the proton target

$\gamma_v p \to \pi^o p,\ \pi^+ n$: P11(1470), D13(1520), F15(1688) for the proton target

Ratio $\dfrac{\gamma_v n \to \pi^- p}{\gamma_v p \to \pi^+ n}$: for the neutron target

The forward and backward production experiments are most suitable to determine helicity-1/2 amplitudes since the helicity-3/2 amplitude cannot contribute due to the helicity conservation at the meson c.m. angles $\theta_\pi \sim 0$ and 180°. The electroproduction experiment at small Q^2 is interesting for a comparison with the real ($Q^2=0$) photoproduction data to see if there are significant differences or not.

The recent exclusive electroproduction experiments are more reliable than the old ones in the identification of particles and better in the momentum resolutions, owing to the extensive use of modern track chambers and various types of Cerenkov counters as well as advanced data handling techniques.

1-1. Kinematics of electroproduction experiment

In this section, I will use the standard notations for the electroproduction kinematics;

$W^2 = M^2 + 2M\nu - Q^2$: squared invariant hadron mass in (γ_v+N) system

$Q^2 = 4EE' \sin^2(\theta_e/2)$: squared virtual photon mass

$\nu = E - E'$: energy transfer

where E, E' are the incident and the scattered electron energy in the laboratory, θ_e the electron scattering angle and M the nucleon mass. The diagram for single meson production process and the definition of meson angles θ^* and ϕ are shown schematically in Fig. 11.

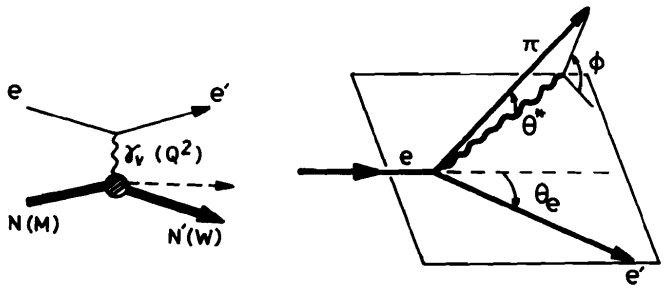

Fig. 11 Meson electroproduction diagram and the definition of meson production angles θ^* and ϕ.

The cross section is given by

$$\frac{d^3\sigma}{dE'd\Omega_e d\Omega^*} = \Gamma t \frac{d\sigma}{d\Omega^*}(\theta^*, \phi)$$

where, $\Gamma t = \frac{\alpha}{2\pi^2}\frac{E'}{E}\frac{K}{Q^2}\frac{1}{1-\varepsilon}$: virtual photon flux factor

$\varepsilon = \left[1 + 2(1 + \frac{\nu^2}{Q^2})\tan^2\frac{\theta_e}{2}\right]^{-1}$: polarization parameter of γ_v

$K = (W^2 - M^2)/2M$

Ω_e: solid angle of scattered electron in lab. system

Ω^*: solid angle of produced meson in (γ_vN) rest system

The virtual photoproduction cross section is expanded in terms of the polarization parameter as

$$\frac{d\sigma}{d\Omega^*} = A + \varepsilon B + \varepsilon C \sin^2\theta^* \cos 2\phi + D\sqrt{2\varepsilon(\varepsilon+1)}\sin\theta^*\cos\phi$$

where A and B correspond to the transverse and the logitudinal photon contribution, C and D are the transverse-transverse and the transverse-longitudinal interference term respectively. These 4 terms are usually decomposed into multipole matrix elements and powers of $\cos\theta^*$.

1-2. New data

The new data contributed to this symposium and those presented since 1978 are tabulated in Table 4. A substantial amount of data taken at Daresbury and DESY have been analysed, and now their final results are available for Q^2=0.5, 1.0, 2.0 and 3.0 GeV^2. As an example, the new data on $\gamma_v p \to \pi^o p$ measured at Q^2= 1.0 by Manchester-Lancaster group[61] are shown in Fig. 12. In this figure, the cross section is plotted against $\cos\theta^*$ and ϕ for W ranging from 1.2 to 1.7 GeV.

Table 4. New data (electroproduction) since 1978

Institute	Q^2 (GeV/c)^2	Channel	W(GeV)	Year	Ref.
Bonn	0.01 - 0.1	π^o backward	1.4 - 1.75	1981	[54]
	0.3	π^+ forward	1.4 - 1.6	1980,'81	[55]
		backward	1.4 - 1.75		
		π^o 30-100°	1.4 - 1.58	1979	[57]
	0.4 - 0.7	π^+ backward	1.4 - 1.83	1981	[56]
Daresbury	0.5	π^o all	1.2 - 1.7	1980	[58]
		π^-/π^+ all	1.3 - 1.7	1978	[59]
		π^-/π^+ all	1.3 - 1.7	1981	[60]
	1.0	π^o all	1.2 - 1.7	1980	[61]
		π^-/π^+ all	1.2 - 1.7	1979	[62]
DESY	0.6	π^o all	1.6 - 1.8	1980	[63]
		η^o	1.5 - 1.6	1980	[64]
	1.0	π^o all	1.7 - 1.9	1980	[63]
		η^o	1.5 - 1.6	1980	[64]
	2.0	π^o all	1.5 - 1.8	1980	[63]
	3.0	π^o all	1.2 - 1.8	1980	[64]

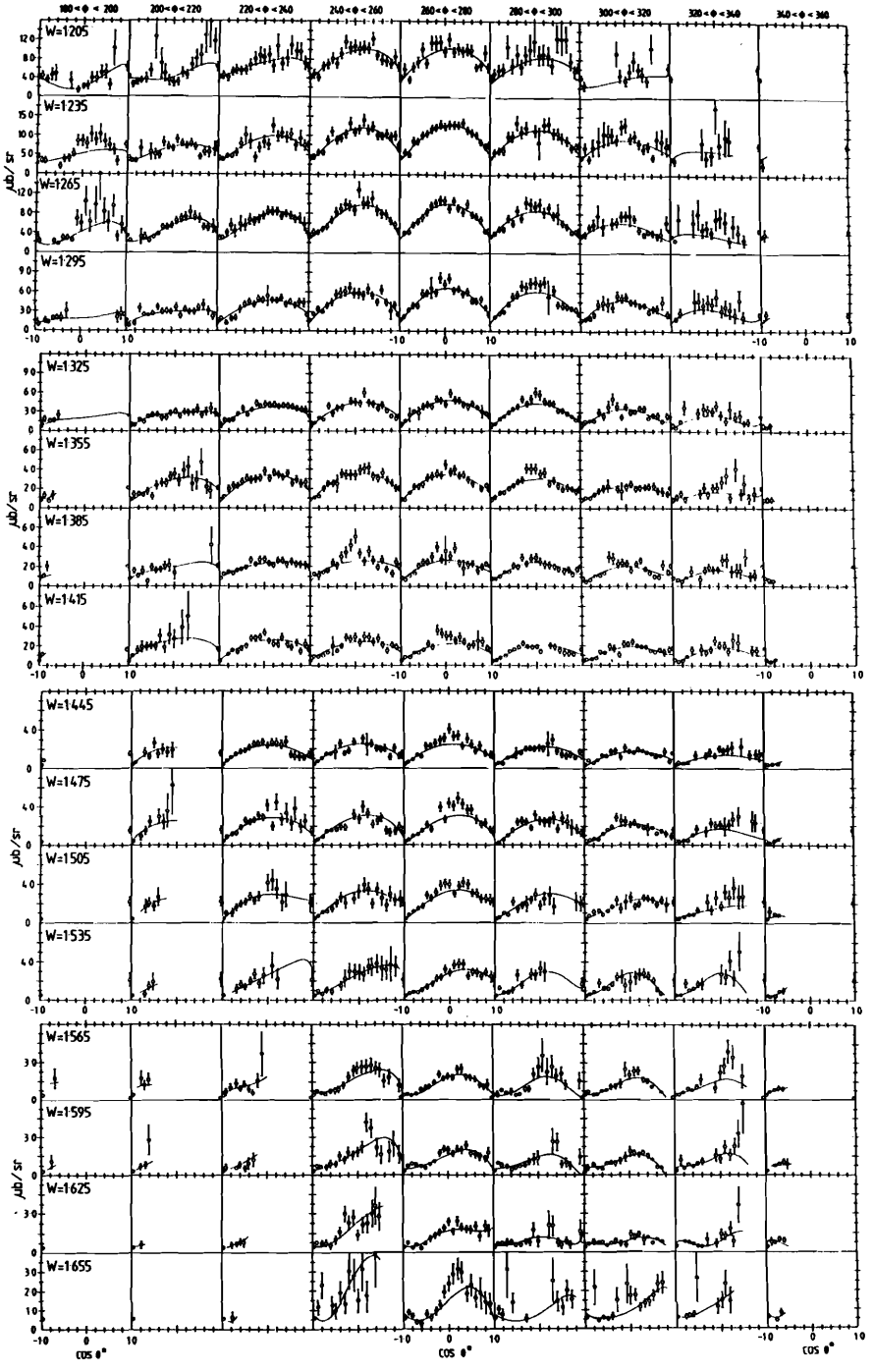

Fig. 12. New cross-section data for $\gamma_V p \to \pi^0 p$ measured by Lancaster-Manchester[61] are shown at various hadron masses(1.2 <W< 1.7 GeV) and meson azimuthal angle ϕ vs. $\cos\theta^*$. The curve represents their fit to the data.

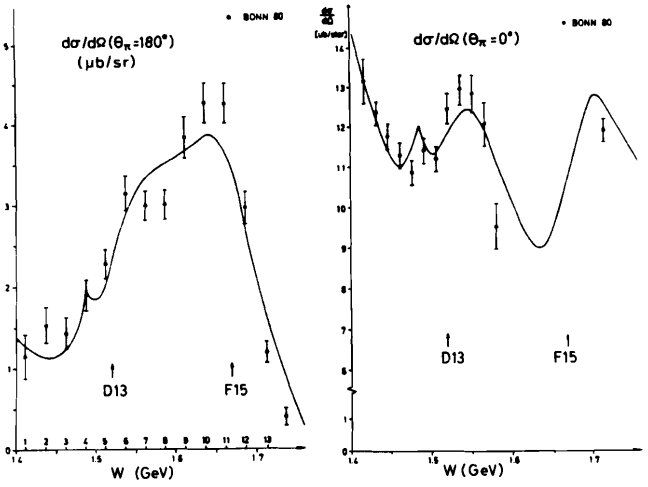

Fig. 13a. New cross-section data for $\gamma_V p \to \pi^+ n$ at $Q^2 = 0.3$ Gev^2 as a function of W measured by Bonn group[55]. The solid curve is a fit to the data by the same group.

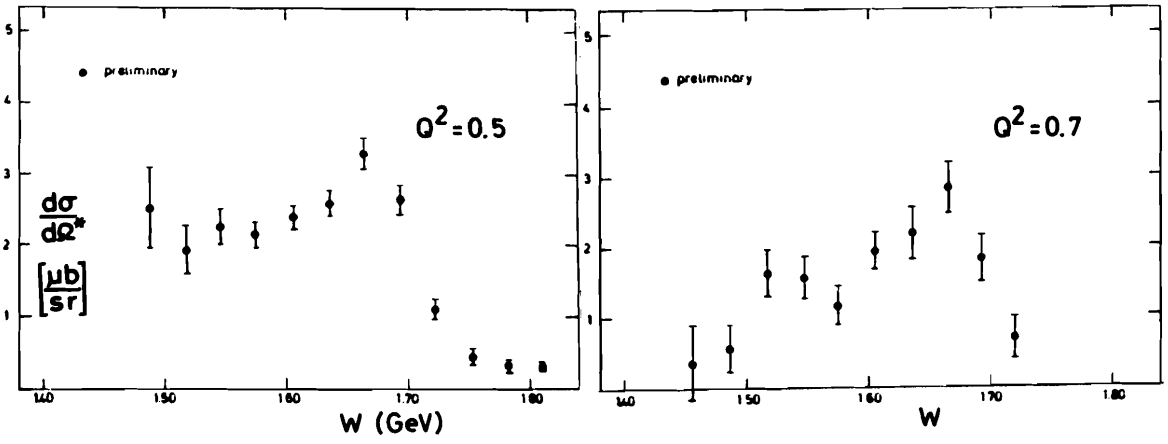

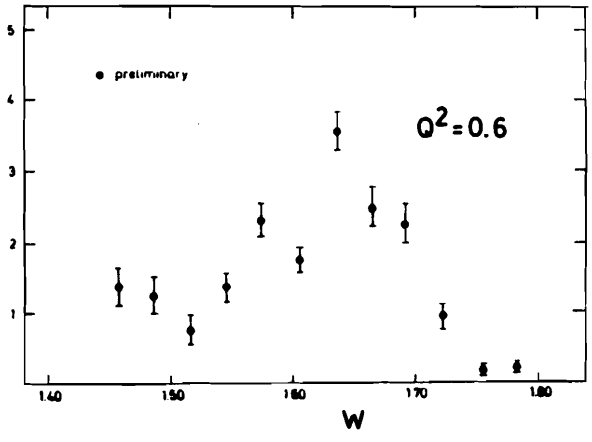

Fig. 13b. New differential cross-section data for $\gamma_V p \to \pi^+ n$ at Q^2 = 0.5, 0.6 and 0.7 GeV^2 at θcm $\approx$ 180° measured by Bonn group[56].

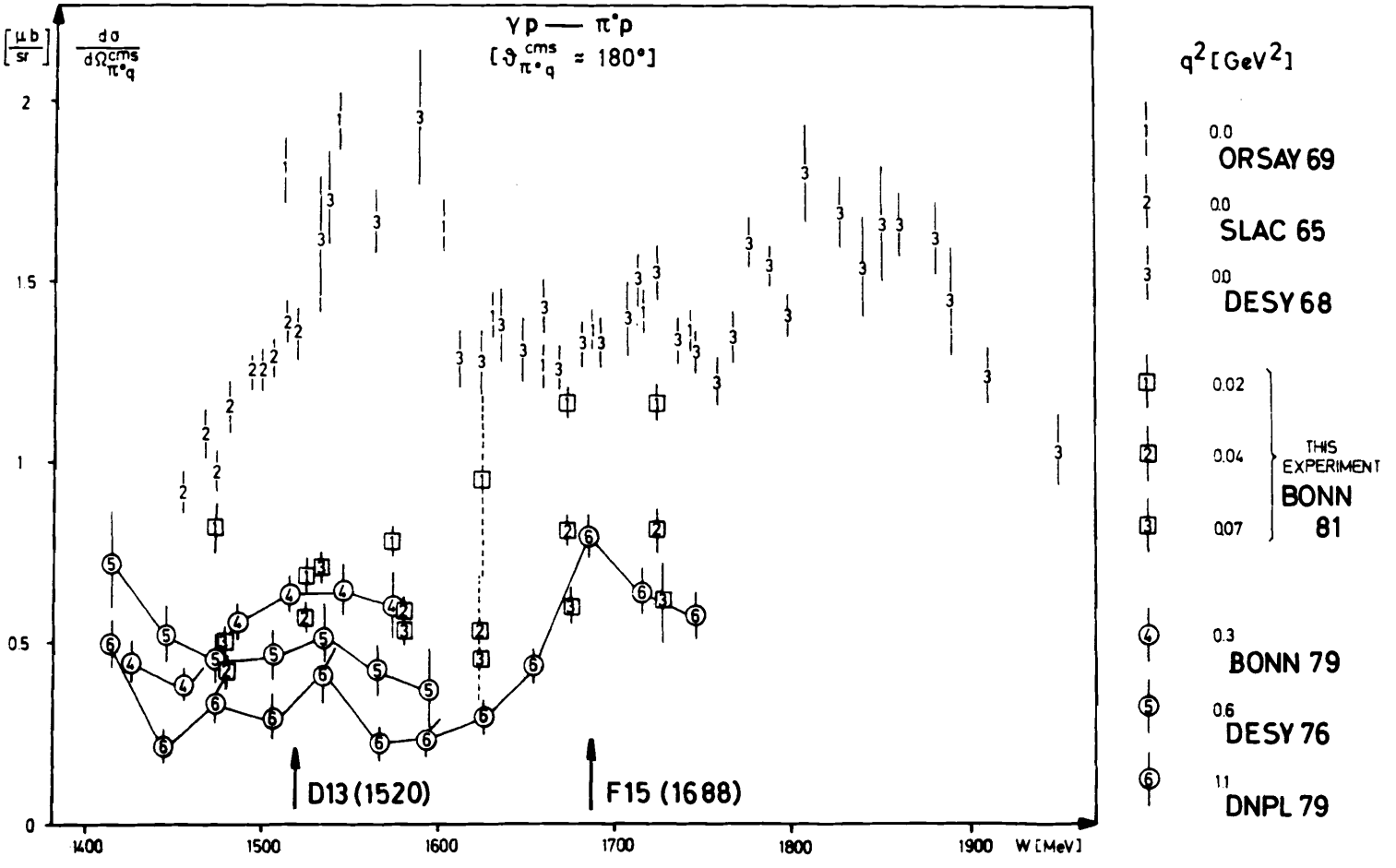

Fig. 14. New backward cross section data on $\gamma_v p \to \pi^\circ p$ at small Q^2 by Bonn group[54] in comparison with the real-photon data [82-84] and those at larger Q^2[57,58,85].

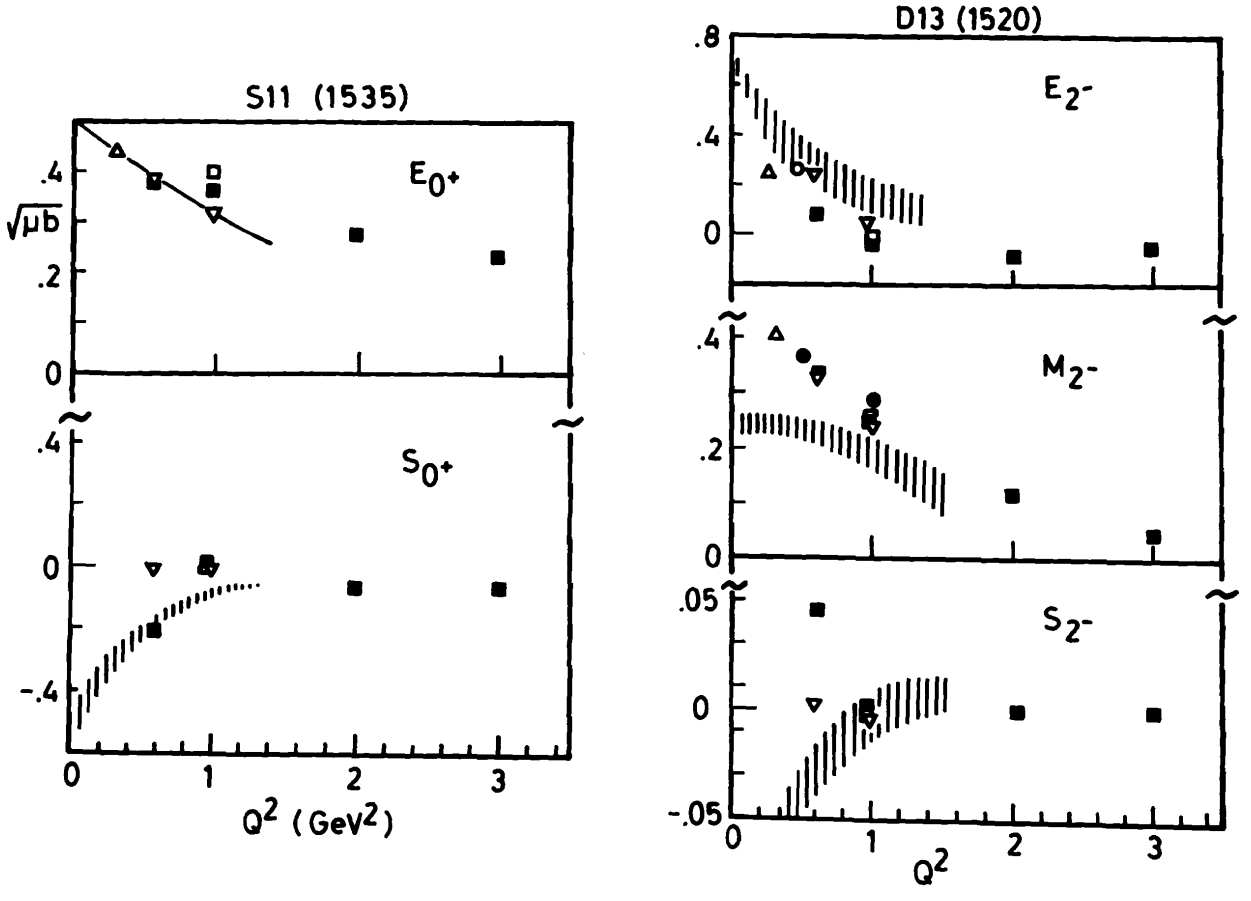

Fig. 15. Multipole couplings for proton target at various Q^2 fitted to π^+, π° and η electroproduction data.

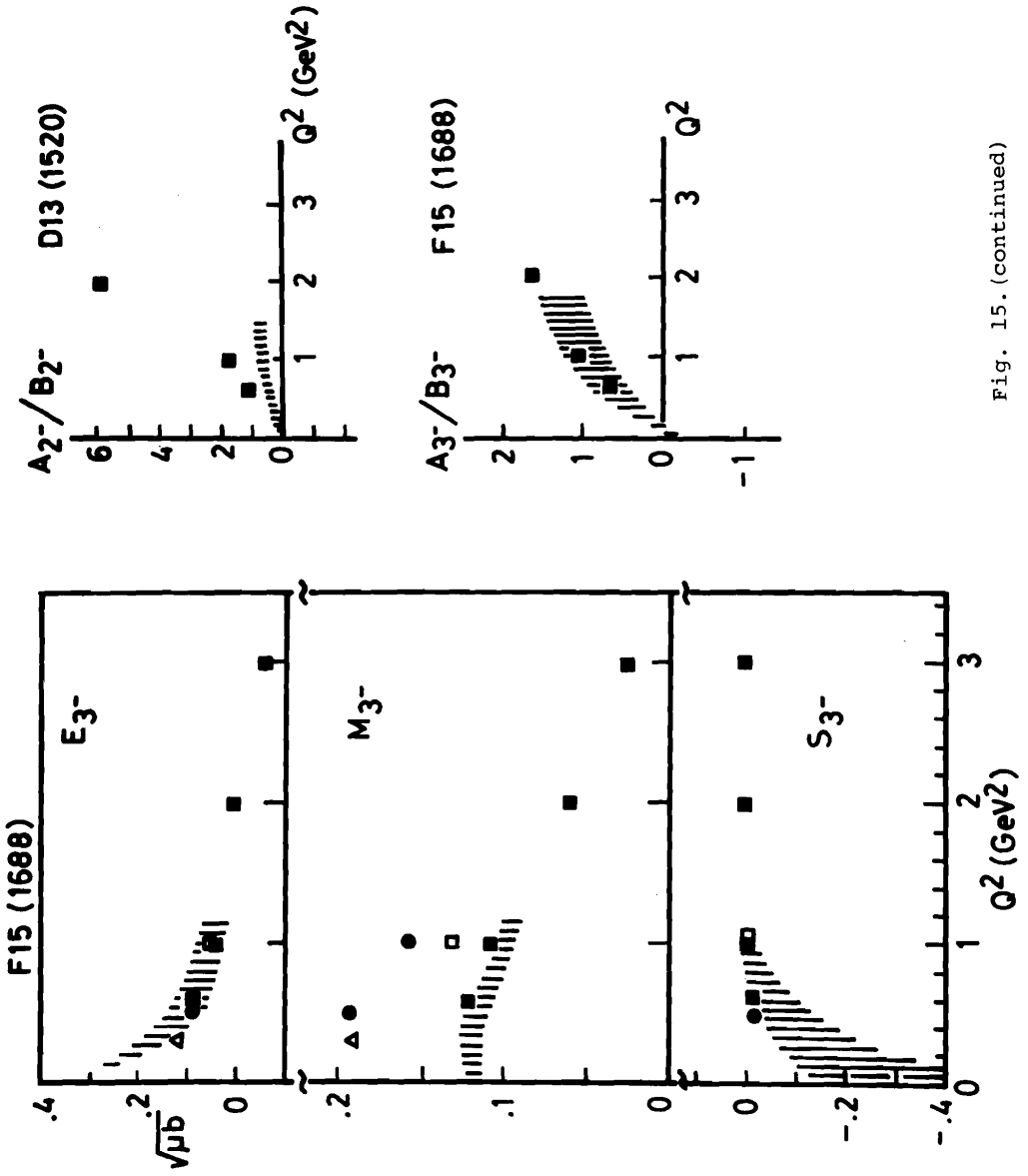

Fig. 15.(continued)

At lower values of Q^2(0.3, 0.5, 0.6 and 0.7 GeV^2), the Bonn group measured π^+ backward and forward production in an energy range of W=1.4-1.75 GeV[55, 56, 57]. They also performed a very small Q^2 experiment of π° backward production aiming for the comparison with the existing Q^2=0 data[54]. These new data are shown in Fig. 13 and Fig. 14. In the latter experiment, a drastic decrease is found in the $\gamma_v p \to \pi^\circ p$ cross section for such a small Q^2 difference. Though the data are in preliminary stage and the estimated systematic errors are rather large ($\sim \pm 30$ %) as shown in Fig. 14, the energy dependence of the data seen at Q^2=0.02, 0.04 and 0.07 is not likely to be changed in final analysis. The peak seen at Q^2=0 corresponding to the 2nd resonance completely disappears, while a re-rise to the F15(1688) resonance still exists. At higher masses (W$\geq$1.7 GeV), however, nothing is not that abnormal. At the present stage, I cannot say much about the reason for this rather puzzling result, but this experimental finding will stimulate interesting discussions about the structure of wave function or the possible existence of strong interference effects in quark scattering inside the nucleon.

2. Multipole analyses and comparison with quark models

2-1. Multipole analysis of new data

The Bonn group[55] made a Walker type analysis for their $ep \to en\pi^+$ and $ep\eta^\circ$ data at $\theta^*=0^\circ$ and 180° for Q^2 =0.3 to derive $A_{1/2}$ amplitudes. In this fit, they varied the $A_{1/2}$ amplitudes of D13(1520) and F15(1688) together with backgrounds, while the S11(1535) and S11(1700) amplitudes were taken from their analysis of η production data. The Lancaster-Manchester group[58,59,60,61,62] analyzed their data by the fixed-t dispersion model originally proposed by Devenish and Lyth (DL 75)[65]. In this case, the electric, magnetic and scalar multipoles are varied for P11(1470), D13(1520), D33(1650) and F15(1688), the couplings to P33(1232) being obtained by a separate analysis and D11(1535), S11(1700) fixed to the results of Wuppertal (1979) analysis[66]. The DL 75 results are used for the rest. They also made a dispersion analysis with their neutron target data by varying amplitudes for P11(1470), S11(1535), D13(1520), S11(1700) and F15(1688) and by using the DL 75 results for others.

In the DESY analysis[74], only resonance couplings to S11(1535), D13(1520) and F15(1688) are varied while others are fixed to the results of DL 75.

I have listed the results of these analyses in Table 5 for the proton target at various Q^2 values, and in Table 6 for the neutron target at Q^2=0.5. The results are also graphically shown in Fig. 15 for S11(1535), D13(1520), F15(1688), with the result of DL 75 analysis for comparison.

From these analyses, transition form factors for the prominent resonances P33(1232), S11(1535), D13(1520) and F15(1688) are well determined, but the coupling to P11(1470) is still ambiguous. An attempt was made by Foster 67 to determine M_1 contribution from the forward π^+ data at Q^2=1.0. He gets the best fit for W<1.41 GeV by forcing the sign of M_1 multipole to change from that observed at Q^2=0. However, this sacrifices the fit at higher masses and thus the helicity-1/2 structures are not reproduced.

2-2. Comparison with the naive quark model

(1) Helicity switching in D13 and F15 amplitudes

This is the famous story about the success of the naive quark model, i.e. leading to the conclusion that the non-relativistic quark model is good as long as the recoil correction for nucleon is not appreciable. In the harmonic oscillator quark model of Copley et al.[68], the D13(1520) and F15(1688) couplings are given as

$$\text{helicity } 1/2 \propto \left(1 - \frac{k^2}{k_o^2}\right) F(k^2) \to 0 \text{ for } Q^2 \to 0,$$

$$\text{helicity } 3/2 \propto F(k^2)$$

where k^2 is the three-momentum of a photon in the Breit frame. If one defines the helicity asymmetry as $A_{1/2,3/2} = (\sigma_{1/2} - \sigma_{3/2})/(\sigma_{1/2} + \sigma_{3/2})$, the asymmetry should increase rapidly from -1 at Q^2= 0 to $\sim$ +1 at $Q^2 \geq 1$ GeV , i.e. the helicity switching. The speed of switching is predicted by various models, hence it is worth to illustrate the present status. In Fig. 16 I plotted the asymmetry

Table 5. Multipole couplings fitted to π^o, π^+ and η electroproduction off proton target

(unit; $\mu b^{1/2}$)

Resonance	Multi-pole	Q^2 (GeV/c)^2 0.3#	0.5†	0.6*	1.0†	1.0*	2.0*	3.0*
P11(1470)	M_{1-}		0.08 - 0.69		0.4 - 0.81			
	S_{1-}		0.0 - 1.37		-0.06 ± 0.06			
D13(1520)	E_{2-}	0.34 ± 0.04	0.37 ± 0.13	0.13	0.08 ± 0.02	-0.04	-0.11	-0.08
	M_{2-}	0.53 ± 0.05	0.53 ± 0.07	0.47	0.43 ± 0.05	0.35	0.17	0.063
	S_{2-}		0.10 ± 0.10	0.06	0.0	0.0	0.0	0.0
S11(1535)	E_{0+}	0.55	0.57§	0.52	0.51§	0.51	0.39	0.32
	S_{0+}		-0.23§	-0.30	-0.14§	0.0	-0.11	-0.10
D33(1650)	E_{2-}		0.23 ± 0.13		0.18 ± 0.07			
	M_{2-}		-0.17 ± 0.03		-0.06 ± 0.02			
	S_{2-}		-0.05 ± 0.05		-0.04			
F15(1688)	E_{3-}	0.13 ± 0.02	0.12 ± 0.10	0.13	0.01	0.07	0.013	-0.084
	M_{3-}	0.30 ± 0.03	0.27 ± 0.01	0.17	0.23 ± 0.02	0.15	0.083	0.038
	S_{3-}		-0.02 ± 0.02	-0.01	0.01 ± 0.01	0.0	0.0	0.0
S11(1700)	E_{0+}	0.44	0.25§		0.21§			

* DESY 79 [74]
† Daresbury 80 [58,75]
# Bonn + Wuppertal 79 [57,66]
§ Wuppertal 79 Fit-3 [66]

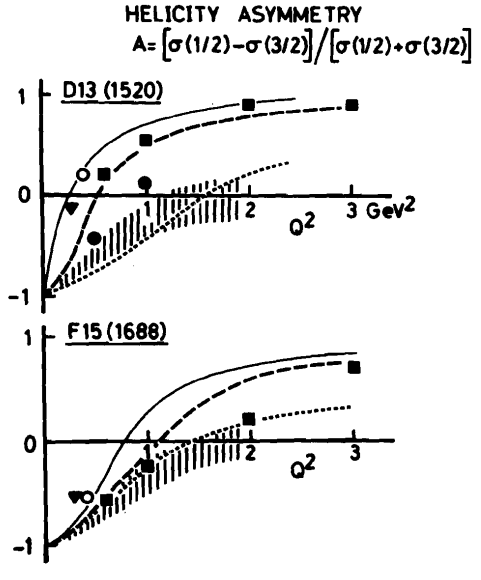

Fig. 16. The variation of helicity asymmetry parameter $A_{1/2,3/2}$ against Q^2 for D13(1520) and F15(1688).

■ DESY 79
○ DARESBURY 74
● ~ 80
▼ BONN 80

——— Ravendal 71[69]
– – – Ono 76[71]
------ Korner et al. 75[70]
|||||||| DL 75[65]

$A_{1/2}$, $S_{1/2}$ taken from various analyses together with theoretical curves obtained from Ravendal 71[69], Korner et al. 75[70], Ono 76[71] and DL 75[65]. All the existing data exhibit a clear switching as seen in the figure. However, when compared to the model calculations, the D13(1520) data follow the rapid switching curve of Ravendal 71 while the F15(1688) is in agreement with Korner et al. 75. For the interpretation of this difference, some[67] speculate that it is attributed to a finite spin-orbit term in the interaction Hamiltonian.

(2) Comparison with single quark transition model (SQTM)

From the determined Q^2 dependence of S11(1535) and D13(1520) multipole amplitudes both belonging to [70,1-] multiplet, one can derive SQTM transition amplitudes between [70,1-] and [56,0-] , as given by Hey-Weyers[72] in 1974. Define the following three amplitudes;

A: quark orbital excitation ($\Delta Lx=1$)
B: quark spin-flig ($\Delta Lz=0$)
C: quark simultaneous spin-orbit flip ($\Delta LZ=1$).

Then one can write:

S11(1535) (in units of $\mu b^{1/2}$)

$$E^p_{0+} = 0.45\left[\frac{1}{6}A + \frac{1}{6}B - \frac{1}{6}C\right] \qquad E^n_{0+} = 0.45\left[-\frac{1}{6}A - \frac{1}{18}B + \frac{1}{18}C\right]$$

D13(1520)

$$E^p_{2-} = 0.48\left[\frac{\sqrt{2}}{6}A - \frac{\sqrt{2}}{12}B + \frac{\sqrt{2}}{12}C\right] \quad E^n_{2-} = -0.48\left[\frac{\sqrt{2}}{6}A - \frac{\sqrt{2}}{36}B + \frac{\sqrt{2}}{36}C\right]$$

$$M^p_{2-} = 0.48\left[\frac{\sqrt{2}}{12}A + \frac{\sqrt{2}}{12}B\right] \qquad M^n_{2-} = -0.48\left[\frac{\sqrt{2}}{36}A + \frac{\sqrt{2}}{36}B\right]$$

The quantity in square brankets gives the production amplitude of resonance and the constant factors are determined by the decay into meson-nucleon system.

The A, B and C amplitudes obtained by Foster[67] and Breuker et al.[55] are tabulated in Table 7 for Q^2 from 0 to 3.0 GeV^2. To study the Q dependence of these amplitudes, the Bonn group tried to separate the variation due to the form factor of the resonance by defining

$$A = A' \, G_D(k^2) \text{ etc.},$$

$$G_D = (1 + k^2/0.71)^{-2}$$

where k is the 3-momentum in the Breit frame. They used the dipole form factor in the Breit frame because the recoil corrections were thought to be minimum in this system. Taking A, B and C amplitudes from Table 6, they obtained A', B' and C' as plotted against k^2 in Fig. 17.

From the quark model calculation, it is expected A' $\sim$ constant, and B' $\sim k^2$. Recently Hey et al. [73] have calculated the C amplitude using the MIT bag model, and their result shows a strong cancellations among various contributions to C. This result agrees quite well with the observed C' as is seen in Fig. 17c in the k^2 range from 0 to 2 $(GeV/c)^2$.

(3) Test of the SQTM

From the A, B, C amplitudes obtained from the data analysis of proton target, we can calculate couplings to various resonances belonging to [70,1-] multiplet. This is done by Foster[67] in 1980 for I=1/2 neutron target multipoles and for other less well known proton target multipoles at Q^2=0.5 and 1.0 GeV . A comparison between the prediction and the data affords a good test of SQTM. In Table 8, the predictions for the neutron target multipoles and for the proton target $D33^+(1650)$ calculated by using the DL 75 fit are listed with the data. Experimental couplings are taken from the Lancaster-Manchester data [60] listed in Table 6. The agreements between the theory and the experiment are good for D13(1520), $D33^+(1650)$, but are poor for both S11(1535) and S11(1700).

The rather qualitative success of the present quark models seems to require

Table 6. Multipole couplings fitted to the neutron target data at $Q^2 = 0.5\ GeV^2$ measured by Lancaster-Manchester[60](unit;$\mu b^{1/2}$)

		Multipole(π^-)		
Resonance	J^P	$E^n(J^P)$	$M^n(J^P)$	$S^n(J^P)$
P11(1470)	1^-		-0.19	0.6
S11(1535)	0^+	-0.11		0.08
D13(1520)	2^-	-0.55	-0.16	0.014
D13(1700)	2^-	-0.034	0.016	0.00
S11(1700)	0^+	0.090		0.097
F15(1688)	3^-	0.039	0.00	-0.013

Proton target multipoles fixed to Devenish and Lyth[65] except $S11^+(1535)$ and $S11^+(1700)$ fixed to Gerhardt fit 3[66].

Table 7. SQTM amplitudes for $[70,1^-]$ at various Q^2[unit;$\mu b^{1/2}$)

$Q^2(GeV)^2$	A	B	C	Source and analysis
0	9.0	3.9	4.2	Litchfield et al.[77]
0.3	6.06	8.22	3.36	#Bonn data, H. Breuker et al.[55]
0.4	4.60	4.60	2.30	#Evangelides et al.[78]
0.5	4.76	6.15	3.21	#NINA '80, Lancaster-Manchester[75]
0.6	3.39	6.41	1.92	*DESY data, R. Haidan[63]
0.5	5.29	4.20	1.95	#Devenish and Lyth[65] fit to
1.0	3.24	3.18	0.95	pre 1975 data.
1.0	2.87	5.96	1.64	#NINA '80, Lancaster-Manchester[75]
1.0	2.28	5.75	0.44	*DESY data, R. Haidan[63]
2.0	1.29	3.77	-0.82	*DESY data, R. Haidan[63]
3.0	1.03	2.45	-1.35	*DESY data, R. Haidan[63]

Foster's calculation[67] of A, B and C from the quoted analyses.

* Calculation of A, B, and C due to R. Haidan[63].

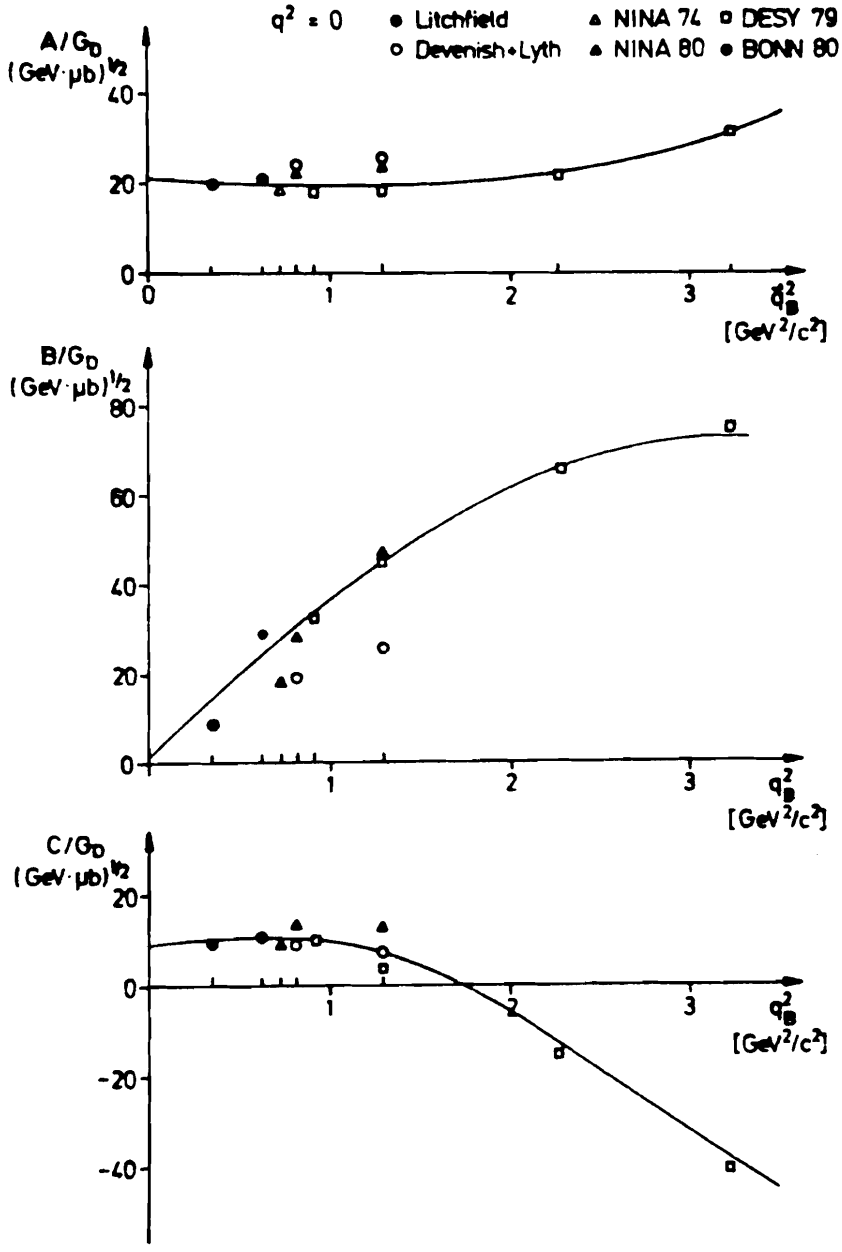

Fig. 17a,b,c. Bonn analysis of the excitation amplitudes $A_{1/2}$ and $A_{3/2}$ for [70,1⁻] multiplet[55] ; orbit flip term A'=A/Gd, spin flip term $B'=B/G_D$ and spin-orbit simultaneous flip term $C'=c/G_D$. The curves are their fit to the data. q_B^2 is 3-momentum transfer squared in the Breit frame.

a more sophisticated theory capable to explain all the available virtual and real photon couplings.

Table 8. Comparison between SQTM and Experiments

$Q^2 = 0.5$ (GeV/c)^2

Resonance	Multipole	Data	SQTM	Ref.
S11(1535)	E^n_{0+}	-0.11	-0.46	[60]
D13(1520)	E^n_{2-}	-0.55	-0.43	[60]
	M^n_{2-}	-0.16	-0.07	[60]
D33(1650)	E^p_{2-}	0.23 ± 0.13	0.20	[75]
	E^n_{2-}	-0.13	-0.20	[60]
	M^p_{2-}	-0.17 ± 0.03	-0.036	[75]
	M^n_{2-}	0.029	0.036	[60]
D13(1700)	E^n_{2-}	-0.034	-0.093	[60]
	M^n_{2-}	-0.016	-0.037	[60]
S11(1700)	E^n_{0+}	-0.09	-0.34	[60]

$Q^2 = 1.0$ (GeV/c)^2

$D33^+(1650)$	E^p_{2-}	0.18 ± 0.07	0.14	[75]
	M^p_{2-}	-0.06 ± 0.02	-0.03	[75]

(4) The first resonance

A theoretical calculation on the $N \to \Delta(1232)$ electromagnetic transition form factor is presented to this Symposium by Jurewicz 76. From a pure dynamical calculation assuming the direct ($\gamma_V N\Delta$) coupling, he succeeded to reproduce the experimentally determined M_1^3 and E_1^3 amplitudes without a phenomenological fit to the data. A plausible interpretation is given as follows; the M_1 excitation to $\Delta(1232)$ occurs promptly through a direct $\pi N \to \Delta$ transition, then followed by a rescattering in the final πN state, and the electric quadrupole excitation E2 being a non-resonant process built up by πN interactions in the final state. In Fig. 18 the calculated transition form factor $G^*_M(q^2)$ divided by the dipole formula approximating the nucleon electromagnetic form factor is given together with the available data. A new data point at $Q^2=3.2$

GeV^2 from DESY 79 [63] is also plotted. The dashed and dash-dotted curves indicate the resonant and non-resonant components, respectively.

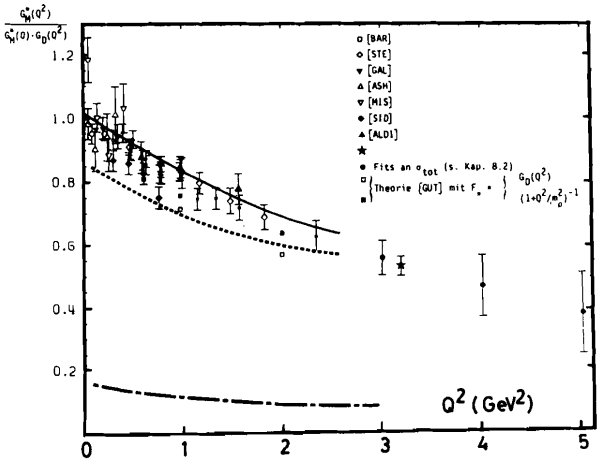

Fig. 18. A new data point from DESY(★) [63] at Q^2= 3.19 GeV^2 and the all available data of the N → Δ(1232) transition form factor G_M^* divided by Gd (dipole form factor) are plotted as a function of Q^2.

Conclusions

I would like to concluded my review on the photoproduction experiments in the resonance region as follows:

(1) Through extensive studies of the single meson photoproduction with real photons, the nucleon resonance couplings are determined up to the 3rd resonance region for the proton and, from an optimistic view, also for the neutron target. To determine the 4th resonance couplings, need more data at high energies.

(2) A quantitative comparison between the experiment and QCD motivated quark models has become possible. Existing quark models predict photocouplings fairly well, however need more detailed study on the spin-orbit interaction, non-spectator excitation etc.

(3) The electroproduction experiment yields more dynamical features of nucleon resonances. From new data, the transition form factors for P33(1232), S11(1535), D13(1520) and F15(1688) are well determined. P11(1470) is still bad.

(4) Only qualitative interpretations are done by the existing quark models. The non-relativistic quark models are good when the correstion due to the nucleon recoil is small, e.g. the helicity switching between $A_{1/2}$ and $A_{3/2}$ amplitudes in the D13(1520) and F15(1683). In general, need more sophisticated model to explain all the available data.

(5) A new π^o electroproduction data at backward suggests a possible existence of an extraordinary effect of the longitudinal wave at extremely small Q^2 (0.04 GeV^2). Needs more experiment for confirmation.

(6) New quark model should consider all the existing data on the πN scatteirng, the real photon couplings, and the transition form factors simultaneously. I think this kind of effort will be profitable for the study of quark many body interaction.

References

1) Barker, I.S., Donnachie, A. and Storrow, I.K., Nucl. Phys. B95(1975)347.
2) Fischer, H., Proceedings 6th Int. Symp. of Electron and Photon Int. 1973 (North-Holland Pub. Comp., Amsterdam-London, 1973).
3) Durwen,E.J. et al., Bonn Univ. preprint, BONN-IR-80-7(1981).
4) Get'man, V.A. et al., contributed paper to the 1980 Int. Conf. on H.E. Physics, Madison.
5) Bussey, P.J. et al., Nucl. Phys. B154(1979)205.
6) Egawa, K. et al., Polarization of Recoil Neutron from Single-Pion-Photoproduction off Protons in the Resonance Region, paper No.202; submitted to this conference.
7) Hampe, P. et al., Bonn Univ. preprint, BONN-IR-80-1(1981).
8) Abrahamian, L.O. et al., contributed paper to the 1978 Int. Conf. on H.E. Physics, Tokyo.
9) Get'man, V.A. et al., contributed paper to the 1979 Int. Symp. on Lepton and Photon Int. at High Energies, Batavia.
10) Fujii, K. et al., Measurement of the Polarized Target Asymmetry on $\gamma p \to \pi^+ n$ in the Third Resonance Region, paper No.225; submitted to this conference.
11) Bussey, P.J. et al., Nucl. Phys. B169(1980)403.
12) Aleksandrov, Yu.et al., Sov. J. Nucl. Phys. 28(1978)344.
13) Althoff, K.H. et al., Bonn Univ. preprint, BONN-HE-79-1(1979).
14) Althoff, K.H. et al., Zeit. Phys. C1(1979)257.
15) Derebchinsky, A. et al., contributed paper to the 1978 Int. Conf. on H.E. Physics, Tokyo.
16) Gorbenko, V.G. et al., contributed paper to the 1979 Int. Symp. on Lepton and Photon Int. at High Energies, Batavia.
17) Kato, S. et al., Nucl. Phys. B168(1981)1.
18) Bussey, P.J. et al., Nucl. Phys. B168(1979)492.
19) Egawa, K. et al., Recoil Proton Polarization in the Reaction $\gamma p \to \pi^0 p$ at Backward Angles, paper No.203; submitted to this conference.
20) Avakyan, R.O. et al., Sov. J. Nucl. Phys. 29(1979)625.
21) Booth, P.S.L. et al., Nucl. Phys. B159(1979)383.
22) Gorbenko, V.G. et al., contributed paper to the 1979 Int. Symp. on Lepton and Photon Int. at High Energies, Batavia.
23) Argan, P.E. et al., Nucl. Phys. A296(1978)373.
24) Abrahamian, L.O. et al., Sov. Phys. Letters 30(1979)696.
25) Takeda, H. et al., Nucl. Phys. B168(1980)17.
26) Fujii, K. et al., Nucl. Phys. B187(1981)53.
27) Kanazawa, K. et al., η Meson Photoproduction from Hydrogen at Photon Energies between 807 and 1007 MeV, paper No.7; submitted to this conference. Inst. for Nucl. Study preprint, INS-Rep-419(July 1981).
28) Walker, R.L., Phys. Rev. 182(1969)1729.
29) Metcalf, W.J. and Walker, R.L., Nucl. Phys. B76(1974)253.
30) Feller, P. et al., Nucl. Phys. B104(1976)219. Revised in Fukushima, M. et al., Nucl. Phys. B130(1977)486.
31) Devenish, R.C.E., Lyth, D.H. and Rankin, W.A., Phys. Letters 52B(1974)227.
32) Moorhouse, R.G., Oberlack, H. and Rosenfeld, A.H., Phys. Rev. D9(1974)1.
33) Knies, G. et al., paper No.957, contributed paper to the 1974 Int. Conf. on H.E. Physics.
34) Crawford, R.L., Nucl. Phys. B97(1975)125.
35) Barbour, I.M. and Crawford, R.L., Nucl. Phys. B111(1976)358.
36) Barbour, I.M., Crawford, R.L., and Parsons, N.H., Nucl. Phys. B141(1978) 253.
37) Arai, I. and Fujii, H., paper No.627. contributed paper to the 1978 Int. Conf. on H.E. Physics. Proceedings of 1979 INS Symposium on Particle Physics in GeV Region, (Inst. for Nucl. Study, Tokyo, 1979), P.87.
Arai, I., Proceedings of 4th Int. Conf. on Baryon Resonances (Univ. of Toronto, Toronto, 1980), p.93.
38) Noelle, P., Prog. Theor. Phys. 60(1978)778.
39) Awaji, N. et al., Energy dependent Partial Wave Analysis on Single Pion Photoproduction, paper No.226; submitted to this conference.
40) Crawford, R.L., Proceedings of the 4th Int. Conf. on Baryon Resonances (Univ. of Toronto, Toronto, 1980), p.107.
41) Cutkosky, R.E. et al., Proceedings of 4th Int. Conf. on Baryon Resonances (Univ. of Toronto, Toronto, 1980), p.19.

42) Ayed, R., Saclay Ph.D. Thesis, CEA-N-1921(1976).
43) Ohta, K., Phys. Rev. 43(1979)1201.
44) Barbour, I.M. and Ponting, D.K., Zeit. Phys. C4(1980)119.
45) Koniuk, R. and Isgur, N., Phys. Rev. D21(1980)1868.
46) Isgur, N. and Karl, G., Phys. Rev. D19(1979)2653.
47) Forsth, C.P., Carnegie-Mellon Univ. preprint, COO-3066-168(1981).
48) Jung, M. et al., Differential Cross Sections of Proton Compton Scattering at Photon Laboratory Energies between 700 and 1000 MeV, paper No.90; submitted to this conference.
49) Ishii, T. et al., Nucl. Phys. B165(1980)189.
50) Kato, S. et al., Recoil Proton Polarization of the Proton Compton Scattering in the Resonance Region, paper No.198; submitted to this conference.
51) Harari, H., Ann. of Phys. 63(1971)432, ibid.Proceedings of 1971 Int. Symp. on Electron and Photon Int. (Lab. of Nucl. Studies, Cornell Univ., Ithaca, 1972).
52) Kölbel, G., Pfeil, W. and Rollnik, H., private communication. Kölbel, G., Diplomarbeit BONN-IR-78-16(1978).
53) Toshioka, K. et al., Nucl. Phys. B141(1978)364.
54) Bellinghausen, H. et al., Electroproduction of π^{o} mesons on Protons at W=1500 - 1750 GeV, q^2= 0.01 - 0.1 GeV^2 and t=1.2 GeV , paper No.73, submitted to this conference.
55) Breuker, H. et al., Electroproduction of π^{+} Mesons at Forward and Backward Directions in the Region of D13(1520) and F15(1688) Resonance, paper No. 138; submitted to this conference.
56) Breuker, H. et al., Backward Electroproduction of π^{+} Mesons in the Second and Third Resonance Regions, paper No.139; submitted to this conference.
57) Rosenberg, M. et al., Bonn Univ. preprint, BONN-IR-79-32(1979).
58) Latham, A. et al., Nucl. Phys. B156(1979)58.
59) Morris, J.V. et al., Phys. Letters 73B(1978)495.
60) Wright, J. et al., Nucl. Phys. B181(1981)403.
61) Latham, A. et al., Daresbury preprint, DL/P 297E(1980).
62) Morris, J.V. et al., Phys. Letters 86B(1979)211.
63) Heidan, R., DESY preprint, DESY F21-79/03(1979).
64) Wriedt, H., DESY preprint, DESY F21-78/01(1978), and Brasse, F.W. et al., Nucl. Phys. B139(1978)37.
65) Devenish, R.C.E. and Lyth, D.H., Nucl. Phys. B93(1975)109.
66) Gerhardt, Ch., Zeit. Phys. C4(1980)311.
67) Foster, F., Proceedings of the 4th Int. Conf. on Baryon Resonances (Univ. of Toronto, Toronto, 1980), p.78.
68) Xopley, L.A. et al., Nucl. Phys. B13(1969)303.
69) Ravendal, F., Phys. Rev. D4(1971)146.
70) Körner, J.G. et al., DESY preprint, DESY-75/57(1975).
71) Ono, S., Nucl. Phys. B107(1976)522.
72) Hey, A.J.G. and Weyers, J., Phys. Letters 48B(1974)69; Hey, A.J.G., Proceedings of Topical Conf. on Baryon Resonances (Oxford, 1976), p.463.
73) Hey, A.J.G., Holstein, B.R. and Sidhu, D.P., Ann. Phys. 117(1979)5.
74) Gerhardt, V., DESY preprint, DESY F21-79/02(1979).
75) Davenport, M. and Morris, J.J., see Foster, F. Ref.[67].
76) Jurewicz, A., N → Δ(1232) Electromagnetic Transition Form Factor and Pion-Nucleon Dynamics at Moderate Energies II , paper No.215; submitted to this conference, and Phys. Rev. D21(1980)695.
77) Litchfield, P.J. et al., Proceedings of Topical Conf. on Baryon Resonances (Oxford, 1976), p.463.
78) Evangelides, E. et al., Nucl. Phys. B71(1974)381.
79) Althoff, K.H. et al., Nucl. Phys. B53(1973)9, B131(1977)1, Phys. Letters 59B(1975)93, 63B(1976)107.
80) Fukushima, M. et al., Nucl. Phys. B130(1977)486. Feller, P. et al., Nucl. Phys. B102(1976)207, Phys. Letters 52B(1974)105.
81) Ukai, K. and Nakamura, T., Inst. for Nucl. Study preprint, INS-TH-136(1981).
82) Delcout, B. et al., Phys. Letters B29(1965)336.
83) DeStaebler, H. et al., Phys. Rev. B140(1965)336.
84) Buschhorn, G. et al., Phys. Rev. Letters 20(1968)230.
85) Alder, J.C. et al., Nucl. Phys. B105(1976)253.
86) Particle Data Group, Rev. Mod. Phys. 52(1980)No.2, Notation and masses of nucleon resonances refer to this reference.

Discussion

G. Karl, Guelph University: I wish to point out that the helicity switching in electroproduction was first noted in the quark model by F. Close & F. Gilman who showed that the cancellations in photoproduction in $A_{1/2}$ could not persist as Q^2 moved away from zero.